NANOOBJECTS & NANOSTRUCTURING

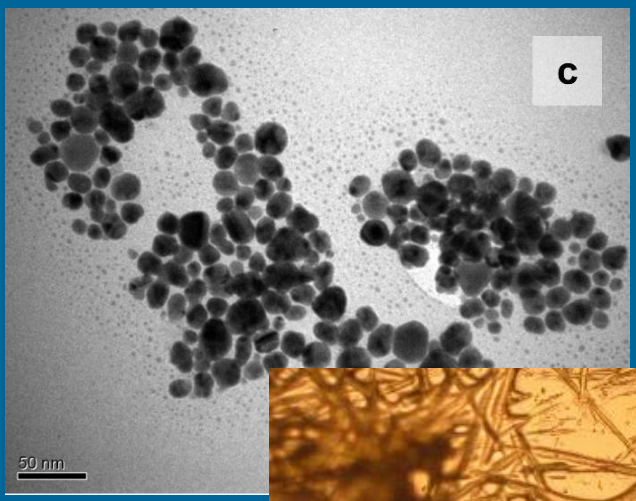

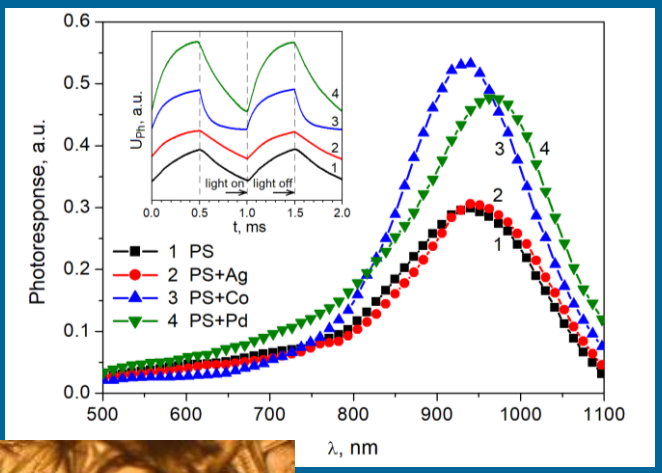

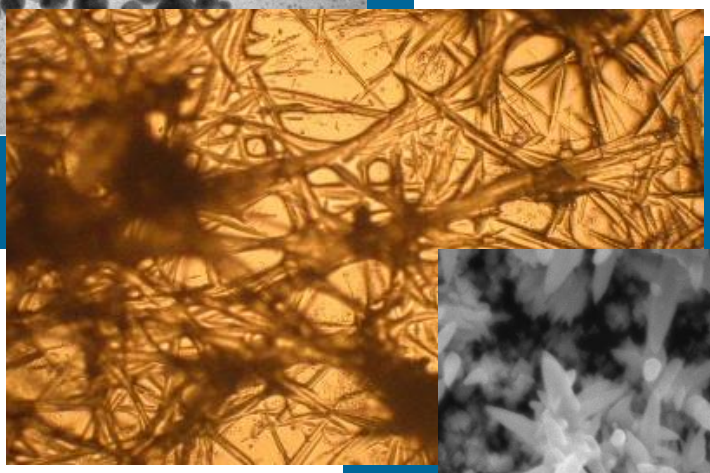

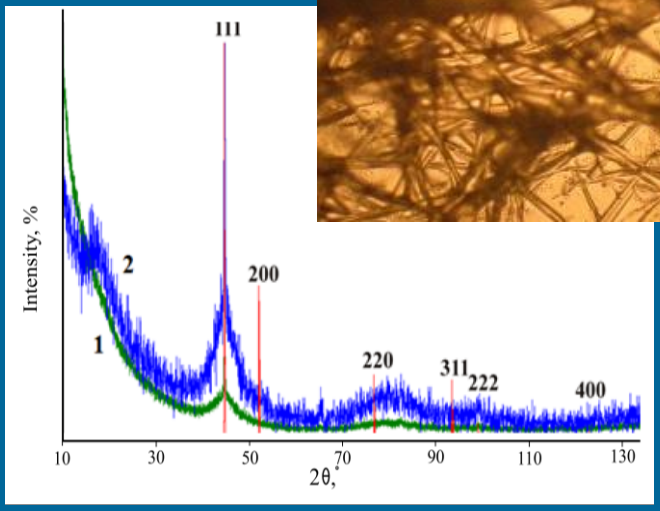

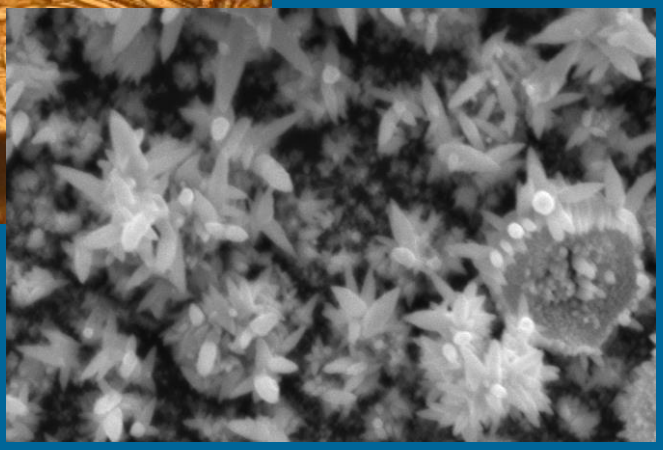

VOLUME I

NANOOBJECTS & NANOSTRUCTURING

COLLECTIVE MONOGRAPH

VOLUME I

NANOOBJECTS & NANOSTRUCTURING

COLLECTIVE MONOGRAPH

VOLUME I

Edited by

Lidiya M. Boichyshyn, CSc
Oleksandr V. Reshetnyak. DSc

Nova Printing Inc.
Mississauga, Ontario, Canada
2022

Nova Printing Inc.
2550 Goldenridge Road
Mississauga, ON, L4X 3S3
Tel: 905-281-3231

Nanoobjects & Nanostructuring. Volume I / Edited by Lidiya M. Boichyshyn and Oleksandr. V. Reshetnyak. – Mississauga, Ontario: Nova Printing Inc., 2022. – 160 + *xviii* p.

This Book is Dedicated
to the 150th Anniversary of
Shevchenko Scientific Society

ABOUT THE EDITORS

Lidiya M. Boichyshyn

Lidiya Boichyshyn, CSc, Docent, Associated Professor of the Department of Physical and Colloid Chemistry of Ivan Franko National University of Lviv (Lviv, Ukraine), Chairwoman of Organizing Committee of International Research and Practice Conference «Nanoobjects & Nanostructuring» (N&N). She is the author of three monographs, 22 patents and more than 300 publications in various journals and conference proceedings. His scientific activity is in the fields of physical chemistry of nanosystems, amorphous metallic alloys, power sources and chemical ecology. She is Deputy Editor-in-Chief of the scientific journal "*Proceedings of Shevchenko Scientific Society. Chemical Sciences*" (Lviv, Ukraine), Valid Member and Deputy Head of the Shevchenko Scientific Society (Lviv, Ukraine).

Contact address:
6 Kyryla & Mefodiya Str., Lviv, 79005, Ukraine
Tel: (+38) (032) 2600–397
E-mail: lidiya.boichyshyn@lnu.edu.ua

Oleksandr V. Reshetnyak

Oleksandr Reshetnyak, DSc, Professor, Laureate of the Borys Paton National Prize of Ukraine (2021), Head of the Department of Physical and Colloid Chemistry of Ivan Franko National University of Lviv (Lviv, Ukraine), Vice-chairman of Program Committee of International Research and Practice Conference «Nanoobjects & Nanostructuring» (N&N). He is the author of three monographs and more than 400 publications in various journals and conference proceedings. His scientific activity is in the fields of physical chemistry of nanosystems, conductive polymers and its composites, electrochemistry of organic compounds. He is a Editor-in-Chief of the scientific journal "*Proceedings of Shevchenko Scientific Society. Chemical Sciences*" (Lviv, Ukraine) and Member of editorial boards of a collection of scientific works *«Visnyk Lvivskogo Universytetu, Seria Khimia»* (Lviv, Ukraine). He is also Valid Member of the Shevchenko Scientific Society (Lviv, Ukraine), member of the Bureau of the Scientific Council of the National Academy of Sciences of Ukraine on the problem of "Electrochemistry» (Kyiv, Ukraine).

Contact address:
6 Kyryla & Mefodiya Str., Lviv, 79005, Ukraine
Tel: (+38) (032) 2600–397
E-mail: oleksandr.reshetnyak@lnu.edu.ua

Chapter 1

NANOFABRICATION OF HYBRID COMPOSITES WITH DIELECTRIC AND SEMICONDUCTOR MATRICES

O. I. Aksimentyeva[1], Yu. Yu. Horbenko[1], I. B. Olenych[1], and G. V. Martynyuk[2]

[1]Ivan Franko National University of Lviv, 79005 Lviv, Ukraine

[2]Rivne State Humanitarian University, Rivne, Ukraine

Corresponding author: olena.aksimentyeva@lnu.edu.ua

Contents

Abstract

The processes of nanofabrication, structure, and properties of hybrid nanocomposites based on dielectric polymer (polymethylmethacrylate, polyvinyl alcohol, polystyrene, etc.) or semiconductor matrices (porous silicon, gallium, or indium selenide, titanium dioxide) with conducting polymers of different nature were studied. The conducting polymer forms its own polymer network inside the host dielectric polymer or semiconductor matrix. It is shown that the concentration dependence of the specific conductivity of composites has a percolation character with a low "percolation threshold" in the range of 1,7–2,5 vol.%. According to EPR-spectroscopy, a dielectric polymer matrix causes significant delocalization of the charge along the macrochains. Semiconductor nanocrystals embedded in the polymer matrix and conducting polymers integrated with porous semiconductor mediums significantly affect the electrical, electrooptical, and luminescent properties of composites causing the shift of spectrum and change of its intensity. The connection between the conditions of synthesis, structure, and properties of materials can cause the expanding functionality of conducting polymer composites for their application in organic electronic devices – gas sensors, organic displays, solar cells, etc.

1.1 Introduction

The rapid development of science and technology led to the emergence of "intellectual" or "smart" polymer nanomaterials, which thanks to multifunctional properties, ease of processing, and environmental stability are extremely promising for modern science-intensive technologies [1–10]. The use of conducting polymer fillers in the structure of "intelligent" material allows the creation of highly efficient devices of a new generation: flexible sensors [3, 6], biosensors [4, 8], supercapacitors [9], antistatic and anti-radar coatings [10], solar cells [5, 7], and organic displays [11]. The principle of operation of these devices is based on the change of electronic properties of conjugated polymers [1, 5, 12–14].

Conjugated polyaminoarenes, in particular polyaniline and its derivatives, have their own electronic conductivity and act as conductive fillers in composites with polymer matrices [6]. Such compounds are characterized by high conductivity and stability [5, 12, 15], simplicity of synthesis, and relatively low cost. These polymers can be considered "synthetic nanometals" with a particle diameter of 10–20 nm and unique electronic, optical, electrochemical, and catalytic properties, including the ability to absorb radioactive rays.

It is known that in polymer-polymer systems, formed by dielectric polymer matrices of different types, conductivity can appear even at low content of conductive filler [6, 14].

The study of percolation phenomena in filled polymer systems is an important fundamental task, as the description of the properties of systems in the vicinity of the critical point opens up prospects for the creation of nanomaterials with predicted functional characteristics.

1.2 Nanofabrication of Conducting Polymers in Dielectric Polymer Matrices

Conducting polymer composites based on conjugated polyaminoarenes – polyaniline and its derivatives are of great interest due to their low relative density, corrosion resistance, good manufacturability (recyclability), and the possibility to control the conductivity. The creation of conducting polymer composites with highly elastic polymer matrices allows for improving the mechanical properties, in particular their flexibility, microhardness, tensile strength, thermoplasticity, etc. [3, 6]. Therefore, macromolecular matrices are intensively searched not only to improve the mechanical properties but also to preserve the features of charge transfer and optical absorption of conducting polymers (CP) in polymer matrices.

The improvement of electrical and optical properties of conducting polymer-polymer composites is achieved at a very low concentration of conducting polymer filler ($\leq$ 5% by volume) and depends on its dispersion degree and filler-matrix interfacial adhesion [6]. At a certain critical concentration value of conductive filler, depending on systems, a jump-like change in properties is observed [6, 9]. That is, the dependence of electrical conductivity (σ) on the volume content of the filler (φ, %) is nonlinear. This is usually an example of a typical percolation transition of a composite from a non-conductive to a conductive state. Herewith, the molecules of the conductive filler or their aggregates form a polymer mesh penetrating the entire volume of the material.

1.2.1 Percolation Phenomena in Polymer-Polymer Nanocomposites

For a scientifical explanation of the complex dependence of conductivity on the content of conductive filler in composite materials (two-phase systems), a "percolation theory" for a continuous medium was formulated. This theory determines the value of the critical volume concentration of the conductive phase φ_C, i.e. the percolation threshold that allows the insulator-conductor transition in stochastic systems [6, 16–19]. The theory of percolation (flow, impregnation) is a mathematical theory used in different fields of science to describe the emergence of infinite connected structures (clusters) in random (stochastic) mediums consisting of individual elements [20].

This theory allows describing processes of diverse nature in conditions when the properties of the system change abruptly with a gradual change in one of the parameters (for example, concentration) [16, 17]. It is used in chemistry to describe the processes of polymerization and analysis of the mutual distribution of phases in different media.

Percolation processes can also lead to self-organization and the formation of nanostructures, including fractals. Many publications [16, 17, 20−22] present various models that characterize the dependence of the percolation threshold on the content of the loading filler.

To describe the concentration dependence of the conductivity of filled heterogeneous composite systems, we can use the basic approaches of the theory of effective environment and the symmetric Bruggeman formula [22]:

$$(1-p)\frac{(\sigma_{DC}-\sigma_m)}{2\sigma_{DC}+\sigma_m}+p\frac{(\sigma_{DC}-\sigma_f)}{2\sigma_{DC}+\sigma_f}=0, \quad (1.1)$$

where σ_f, σ_m, σ_{DC} − electrical conductivity of the filler, polymer matrix, and composite, respectively; p − the effective volume content of the filler.

The main equation of percolation theory (Kirkpatrick's model or scaling law) in filled polymer systems, which reflects the dependence of electrical conductivity (σ) on the bulk content of the filler (φ) after the percolation threshold is the dependence:

$$\sigma \infty (\varphi - \varphi_c)^t, \quad (1.2)$$

where φ − the volume fraction of filler; φ_c − the percolation threshold, i.e. the lowest content of filler at which a continuous cluster of conductivity is formed from particles under the condition $\varphi > \varphi_c$; t − the critical conductivity index.

To determine the critical parameters, a logarithmic dependence $\lg \sigma - \lg(\varphi - \varphi_c)$ is constructed. The slope of the obtained line gives the value of "t". For a three-dimensional system, the universal constant t acquires values of 1.6 −2.06, which is mainly dependent on the topological dimension of the system and not dependent on the structure of the particles forming the clusters and their interaction [20–23].

The study of percolation phenomena in filled polymer systems is an important task because the description of the properties of the systems near the critical point opens the perspectives for the creation of nanomaterials with predicted functional characteristics. In this work, the electrical properties of polymer-polymer composites based on dielectric polymer matrices, namely polymethyl methacrylate (PMMA), a copolymer of styrene with malein anhydride − styromal (St-MA), polyvinyl alcohol (PVA), polyacrylic (PAA) and polymethacrylic (PMAA) acids, ED-20 epoxy matrices, and conducting polymer fillers – poly-ortho-toluidine (PoT), poly-ortho-anisidine (PoA) and polyaniline (PAn) were studied [3, 6, 10, 13, 14, 24–26].

It is shown that the concentration dependence of the specific conductivity on the content of fillers has a percolation character (Fig. 1.1) with a low "percolation threshold", which depends on the nature of the polymer matrix and conducting polymer (Table 1.1). Increasing the filler content leads to a sharp transition from the non-conductive to the conductive state (there is a phase transition insulator-conductor). In this case, all the filler particles are completely delocalized throughout the polymer matrix and become conductive, and the formed composite has the maximum conductivity. It was found that composites

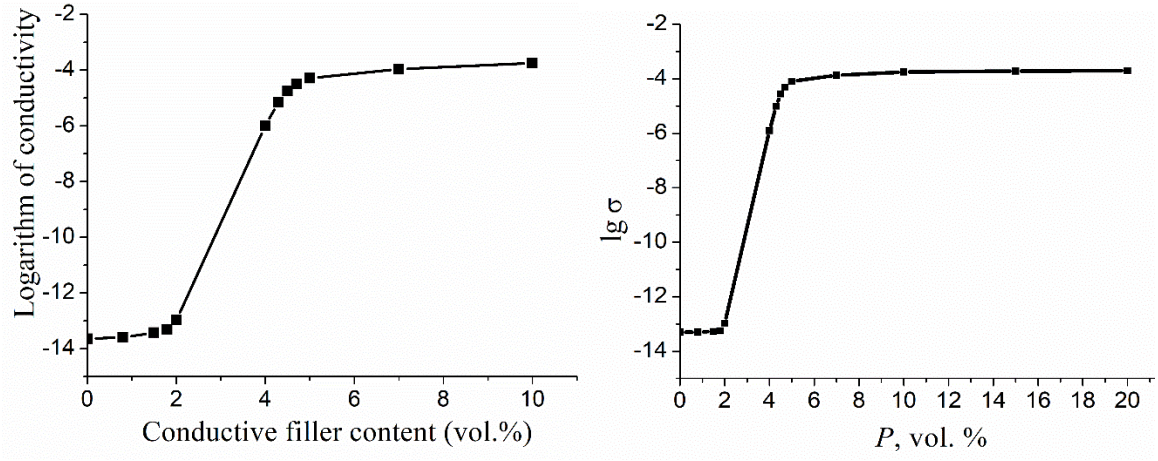

Figure 1.1 Dependence of logarithm of specific conductivity on the content of conductive filler for: (*a*) PVA-polyaniline composites, φ_c = 2.3 vol. %; (*b*) PMMA-PAn, φ_c = 2.0 vol. %

Table 1.1 Percolation parameters of polymer composites with conducting polymer fillers

Polymer matrix	Conducting polymer filler	Percolation threshold φ, vol. %	Critical index of conductivity, t
PVA	PAn	2.1	1.75
	PoT	2.8	1.58
	PoA	1.7	1.88
PMMA	PAn	2.0	1.43
	PoT	3–4	1.48
PAA	PoT	2.3	1.38
St-MA	PoT	10	2.53
	PAn	8.4	2.67
	PoA	8.0	2.56
ED-20	PAn	2.5–5	–

based on the investigated polymer matrices are characterized by low values of the percolation threshold, which are typical for composites with a conductive polymer phase. The calculated values of the critical index of conductivity are in the range of 1.4–2.6, which is characteristic of a three-dimensional system [27]. This constant is mainly dependent on the topological dimension of the system and not dependent on the structure of the particles forming clusters and their interaction.

At the same time, the value of $t \approx 2$ is observed for many two-phase materials. Significant deviations of this value for composites based on the StMA matrix ($t \approx 2.58$–2.9) can be caused by several reasons: contact phenomena, in particular, if tunnel contacts are

realized between the conductive elements of the material, instead of ohmic [28], different morphology, and different specific surface of the material [29]. The deviation of the critical index "*t*" from universal values can be explained by the peculiarities of composites formation in "*in situ*" polymerization conditions, when the conductive filler is formed directly in the dielectric polymer matrix, and by the presence of anisotropic forms of conductive filler [30].

1.2.2 Features of Charge Transfer in Conductive Polymer Composites

The study of the influence of the polymeric matrix on the regularities of charge transport in nanosystems with conductive polymers is an interesting scientific task due to the possibility of their practical application. We chose the PMMA-PAn polymer nanocomposites obtained from polymer "blends" in a common organic solvent [6, 13, 14]. It was found if the content of PAn becomes higher than 2 vol. %, the conductivity value of the PMMA-PAn composite exceeds the conductivity of the PMMA matrix by 8–9 orders of magnitude, and remains almost constant. It is interesting that the conductivity of the PMMA-PAn composite with a filler content of 2–15 vol. % slightly exceeds the conductivity of pure PAn (Table 1.2). We assume that high values of the specific conductivity (σ) exceeding the percolation threshold for PMMA-PAn composites are caused by the formation of their own conductive network inside the host polymer. Thus formed continuous conductive phase is uniformly distributed over the entire volume of the polymer composite – a continuous conductivity cluster is formed [16–18].

As shown by B. Wessing and co-authors [31], the conductivity in thermally compressed PAn composites doped with d,l-camphorosulfonic acid with PMMA, containing 40 % PAn, may be higher than that of pure PAn. A probable cause of this phenomenon may be the additional doping of the polyaniline by PMMA functional groups near the melting point. On the other hand, the dielectric polymeric matrix can affect the degree of coupling of the conductive polymer structure by orienting the macrochains in one direction forming 1D structures [32]. The presence of structures of this type ensures the preservation of the physicomechanical properties of high-polymer matrices without disrupting the semiconductor nature of the conductivity of the conjugated polymer. Moreover, it sometimes even enhances charge transport, affecting its electronic structure, which leads to changes in the concentration of polaron charge carriers. Perhaps, in this case, a structural matrix effect is appeared, which consists of the ability of the polymer matrix to influence the length and chemical structure of polyaminoarene chains, including their spatial structure. Using ESR

Table 1.2 The dependence of the specific conductivity on the content of the polymeric filler for PMMA-PAn composites

ω, vol. % of PAn	0	1	2	4	10	20	100
$\sigma_{298}\cdot 10^6$, S·m^{-1}	10^{-8}	7.03	81.2	52.8	27.6	2,16	3,60

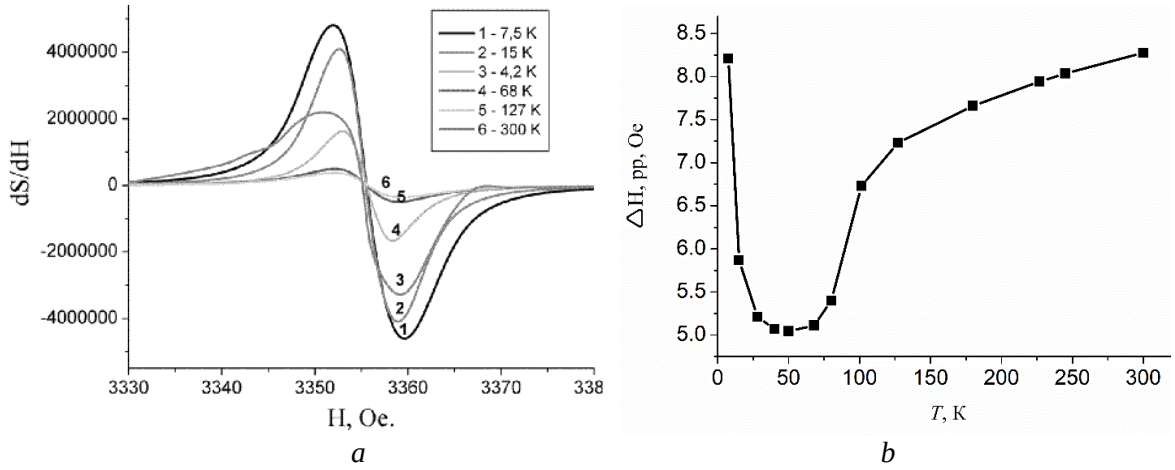

Figure 1.2 (*a*) ESR spectra for PMMA-PAn (10 vol. %) at different temperatures; (*b*) Dependence of signal width ΔH_{pp} (distance between peaks) on temperature for PMMA-PAn (10 vol. %)

spectroscopy in the range T = 4.2−300 K it was established that PMMA-PAn composites give a clear EPR signal at room temperature with a g-factor value of 2.0025 ± 0.0002 (Fig. 1.2, *a*). According to the analysis of the ESR temperature dependence, it can be assumed a significant delocalization of charge carriers along the PMMA dielectric polymeric matrix causes increased values of the specific conductivity (Table 1.2). This is also evidenced by the change in the shape of the ESR signal, namely its significant extension − the distance between the peaks ΔHpp increases to 5.05−8.29 Oe for the PMMA-PAn composite (Fig. 1.2, *b*) compared to the unfilled PAn (3.1−3.4 Oe) [31, 33, 34].

Therefore, it was established a strong interaction between the PMMA polymer matrix and the PAn filler, which is manifested in the low percolation threshold values for these composites explained by the formation of a spatial conductive network. On the other hand, the dielectric polymeric matrix can affect the structure of the conjugated polymer, and, therefore, the number of unpaired spins corresponding to the charge carrier concentration. The results of ESR spectroscopy confirmed this assumption. The electronic structure of the material significantly changed because of PMMA-PAn formation may indicate the formation of a composite with a molecular degree of dispersion, in other words, a nanocomposite.

Among industrial polymer matrices, polystyrene (PS) attracts special attention due to its excellent mechanical properties, transparency in visible spectral range, easy processing, and availability [36–44]. PS-CP composites are used in various industries for the production of antistatic screens, conductive coatings on the surface of various natures, thin-film chips, as well as sensors for the detection of ammonia, and hydrogen sulfide [38, 39]. The growing interest in protection against electromagnetic interference using of polymer-polymer composites based on CP is due to the increased variety of commercial, military, and scientific electronic devices. It is shown [40] that the polymer complex PAn doped with dodecylbenzene sulfonic acid (DBSA) and polystyrene-polybutadiene-b-styrene copolymer can be used as a coating for protection against electromagnetic interference in the 50–60 Hz and 1–100 GHz bands.

Currently, there are many methods of synthesis of conductive composites based on PS and polyaminoarenes [39–44]. Despite the variety of ways to obtain such polymer composites, they nevertheless have some drawbacks − complex, long, multi-stage process technology. Synthesized composites are in the form of a dispersed powder, which makes it impossible to form films and conductive coatings by irrigation or inkjet printing on work surfaces. Besides, it causes an uneven distribution of polyaminoarene in the matrix of PS, heterogeneous structure and low sedimentation stability of the system, and low conductivity of composites. The use of polyaniline as a conductive polyaminoarene reduces the choice of conductive polymeric fillers and narrows the scope of such composites in modern industry. A new nanotechnological approach in the formation of polystyrene composites with polyaminoarenes is *in situ* polymerization when conjugated conducting polymer is synthesized directly in the polymer matrix solution, i.e. aniline polymerizes to polyaniline [40, 43]. This leads to higher dispersion and uniform miscibility of PAn nanoparticles in the polymer matrix. *In situ* polymerization of aniline in the presence of $(NH_4)_2S_2O_8$ is descrybed in a lot of research. The use of PoT as a filler in the PS matrix is little known, in particular, copolymers poly(aniline-co-o-toluidine) nanocolloidal particles in aqueous poly(styrene sulfonic acid) matrix (PPS) [37]. We used aminoarenes – *o*-toluidine and aniline, which differ in the presence of a substituent on the benzene ring, as monomers for the formation of a conductive polymer filler in the PS dielectric polymer matrix. In the *o*-toluidine molecule, the presence of methyl substituent in the *ortho* position to the amino group determines the hydrophobic properties of aminoarene and in traditional solvents in contrast to unsubstituted aniline.

In the process of nanofabrication polymer-polymer composites by the *in situ* polymerization method, various mechanisms of formation and self-organization of the conductive phase of conjugated polyaminoarenes are possible. Depending on the nature and initial concentration of the monomer in the reaction mixture, different morphological features of the formed film can be observed (Fig. 1.3). The polystyrene matrix (Fig. 3, *a*) is characterized by excellent homogeneity, smooth morphology, and absence of agglomerates or crystalline formations. In the process of oxidative polymerization of aniline in the PS matrix, a formation of PAn nanofibrils which formed a continuous polymer network takes place

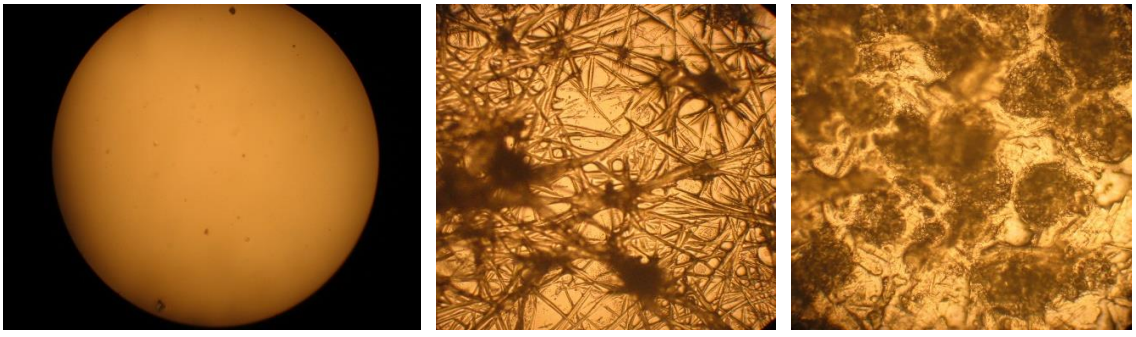

a *b* *c*

Figure 1.3 Microphotos of films: (*a*) PS and composites (*b*) PS-PAn-TSA, *(c)* PS-PoT-TSA. Filler content 10 wt. %, magnification ×150, film thickness 0.2 ± 0.02 mm

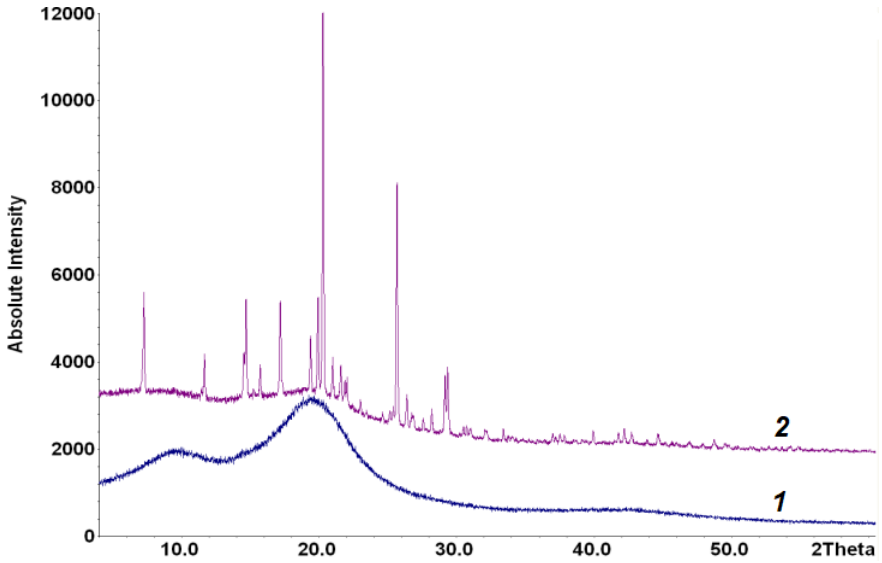

Figure 1.4 X-ray diffraction patterns of PS (*1*) and PS-PoT-TSA (*2*) composite (10 wt. %)

(Fig. 3, *b*). The formation of PoT network in PS matrix is observed at the low concentration of *o*-toluidine in the reaction mixture (3–5 wt. %). The highly ordered conductive regions of the PoT filler embedded in the matrix of polystyrene are observed at higher monomer concentrations (Fig. 3, *c*).

Investigation of the structure of composites by X-ray powder diffraction method showed that the original PS is practically amorphous, and the diffraction pattern of the PS has a wide peak at $2\theta = 19^{\circ}$ (Fig. 1.4). A calculated average apparent crystallite size is D = 9.3±1.3 Å. In PS-PAn composites, additional polyaniline peaks are observed at $2\theta = 14.5°$, 19.7°, 25.3°, and 27.1°, which are almost completely leveled at 7 wt. % polyaminoarene content [43]. The composite PS-PoT-TSA is characterized by a predominantly ordered structure and, accordingly, a high degree of crystallinity, while the content of the amorphous component is low. A high level of structure ordering in PS-PoT-TSA composites is connected with the crystalline structure of the filler PoT-TSA confirmed in [46, 47]. The spatial and geometric similarity of fragments of PoT and TSA leads to the formation of an ordered and more compact structure of the doped polymer.

Polystyrene has poor conductivity, the resistivity is at the level of 10^{14}–10^{15} Ohm·cm [46]. At a low concentration of polymer filler (near 2 wt. % PAn-TSA or PoT-TSA) nanofabricated in PS matrix the specific volume resistance falls in 10–12 order and demonstrates percolation behavior inherent in nanostructured systems [18, 46]. After reaching the percolation threshold (0,75 % for PS-PAn composites [43]) the resistance of PS composites with conducting polyamenoarenes is significantly reduced (Table 1.3). The reduction of the resistivity of the composite is proportional to the concentration of conducting polymer filler. At the content of conducting polymer filler in PS-PoT-TSA composite near 20 wt. %, a value of specific volume resistance at room temperature ρ_{293} = 6,8 Ohm·cm, specific conductivity $\sigma_{293} = (1.5\pm0,2)10^{-1}$ S/cm. For PS-PAn-TSA composite, the values of conductivi-

Table 1.3 The parameters of conductivity of polystyrene-polyaminoarene composites

Sample	Monomer concentration, M	Filler content, wt. %	σ_{293}, S/cm	ρ_{293}, Ohm·cm	E_a, eV
PS-PAn-TSA	0.01	2	0.023	44.1	0.93 ± 0.01
	0.03	6	0.027	37.3	0.63 ± 0.01
	0.05	10	0.029	33.9	0.71 ± 0.02
	0.075	15	0.033	30.5	0.81 ± 0.02
	0.10	20	0.037	27.1	0.37 ± 0.01
PAn-TSA		100	0.043	23.7	0.08 ± 0.01
PS-PoT-TSA	0.01	2	0.049	20.4	0.73 ± 0.02
	0.03	6	0.059	16.9	0.62 ± 0.04
	0.05	10	0.073	13.6	0.57 ± 0.01
	0.075	15	0.098	10.2	0.44 ± 0.01
	0.10	20	0.150	6.8	0.40 ± 0.03
PoT-TSA		100	0.294	3.4	0.047 ± 0.003

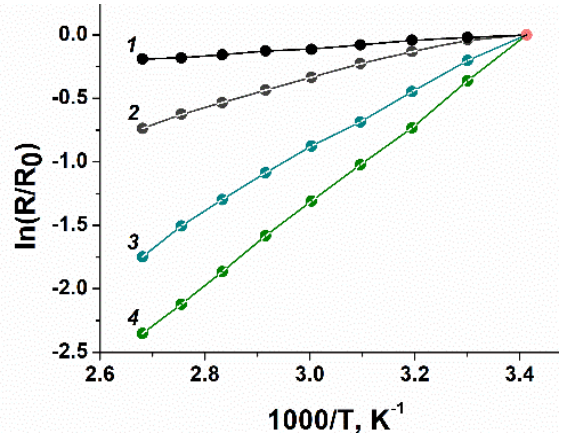

Figure 1.5 Temperature dependence of normalized resistance: PoT-TSA (*1*), PAn-TSA (*2*), PS-PoT-TSA (*3*), PS-PAn-TSA (*4*) at 10 wt. % content of polymer filler

ty are less (4,3±0,2) 10^{-2} S/cm at the same content of polymer filler (Table 1.3). Structural and morphological features of the composites may explain it.

The temperature dependence of the normalized resistance of the polymer fillers and composites as $(R/R_0) = f(1/T)$ is linear in the temperature range 303–373 K (Fig. 1.5). The activation energy of conductivity E_a was calculated by the equation:

$$\rho = \rho_0 \cdot \exp\left(E_a / 2kT\right), \tag{1.3}$$

where ρ – specific electrical resistance, k – Boltzmann constant, T – temperature. E_a was found 0.047 ± 0.003 eV for PoT-TSA and 0.08 ± 0.01 eV for PAn-TSA fillers. The calculated activation energy of charge transport for PS-PoT-TSA composites decreases with content of filler from 0.73 ± 0.02 eV (2 wt. %) to 0.57 ± 0.02 eV (5 wt. %), and 0.40 ± 0.03 eV (20 wt. %). It is similar to PS-PAn-TSA composites (Table 3). To conclude, the dielectric polymer matrix causes a significant increase in activation energy for both fillers – PAn-TSA and PoT-TSA.

TSA-doped poly-*ortho*-toluidine as a conductive filler significantly increases the electrical conductivity of polystyrene-polyaminoarene composites due to the formation of a highly ordered structure. The spatial and geometric similarity of fragments of PoT and TSA leads to the formation of an ordered and compact structure of the polymer filler in a polystyrene matrix.

Synthesized polymer-polymer composites can be used for various purposes, in particular, the production of antistatic screens, conductive coatings on the surface of various natures, thin-film chips by the inkjet printing, or the watering of the composite material on the substrate (work surface). This method allows you to apply the composite on a plastic or other substrate in the form of paint, which dries quickly. One of the most interesting applications of conducting polymer nanocomposites is the creation of chemical sensors sensitive elements [47–50], especially, gas sensors for monitoring the toxic gases in the environment and industry.

1.2.3 Formation of Flexible Elements of Gas Sensors

Nowadays, gas-sensitive films based on conducting polymers (PAn and its derivatives, polyoxythiophenes, etc.) are one of the most promising sensor media. The properties of these polymers are based on chemical redox reactions and provide various mechanisms for the generation and transformation of electrochemical, electrical, or optical signals [47–58]. The creation of composite sensor media based on conducting polymers and dielectric polymer matrices allows to combine of the advantages of each of the components – the sensitivity of conjugated polymers to the action of gases with the flexibility, lightness, and recyclability of polymer matrices. Moreover, such sensor elements can operate at normal temperatures. Nanocomposites based on conjugated polyarenes are quite sensitive to gases, released because of food freshness losses (NH_3, H_2S [49, 57-59]), vapors of organic compounds [60], chemical components of military explosives, and gases released in their storage (NO_2, SO_2, etc.) [61].

Composites of conducting polymers with dielectric polymer matrices are usually obtained by mixing a conducting polymer filler with non-conductive highly plastic polymers (PMMA, PVA, PS, cellulose derivatives) followed by thermal pressing [61, 62]. The most promising method of providing elasticity and thermal-plasticity of polyaminoarenes is the creation of polymer composites in which components mix at the molecular level. This method is used to obtain polymer-polymer composites with an ordered structure, as well as nanosized composites from polymers insoluble in water and in most organic solvents. We

used such approaches to polymerize aminoarenes in a polymer gel (PVA, PAA, PMAA) whose macromolecules act as "soft" templates [6]. It was shown that the interaction of the functional groups of the polymer matrix with the amino groups of the polymeric filler is possible [14]. The interaction affects the kinetics of polymerization and all the physical, chemical, and mechanical properties of composites [6, 14, 63]. It was found that the mass fraction of 0.35-1.05 % of the monomer in the initial composition is optimal [64].

Obtaining the free flexible films of a composite of conjugated polyaminoarene and a highly elastic polymer matrix was carried out by oxidative polymerization of 0.01–0.025 M aminoarenes solution at the equimolar content of oxidizer (ammonium persulfate) in an aqueous gel of PVA (PAA or PMAA) with concentration 0.125–5 w. % during 24 h. The films were formed by pouring the composition on the surface of Teflon or glass with subsequent monolithization of the film at room temperature over 6–8 h and finally at 331–333 K for 1 hour. After separation from the substrate homogeneous flexible sensitive films were obtained [65].

In the process of oxidative polymerization of aminoarenes within 24 hours at a monomer : oxidizer ratio of 1:1 almost complete (95–98 %) conversion of the monomer is achieved. It corresponds to the 4.5–15 w. % content of the conductive polymer in the final composite. The obtained polymer-polymer composites form flexible, highly elastic "free" films (Fig. 1.6, *a*, *d*) easy for preparing indicator tapes. The structure of the film composites based on PVA and polyaminoarenes is sufficiently homogeneous and compact and at the same time, its globular nature is preserved (Fig. 1.6, *b*, *c*, *e*). Composites with matrices based on polymer electrolytes (PAA, PMAA) form not only flexible but also transparent "glass-like" films (Fig. 1.6, *f*).

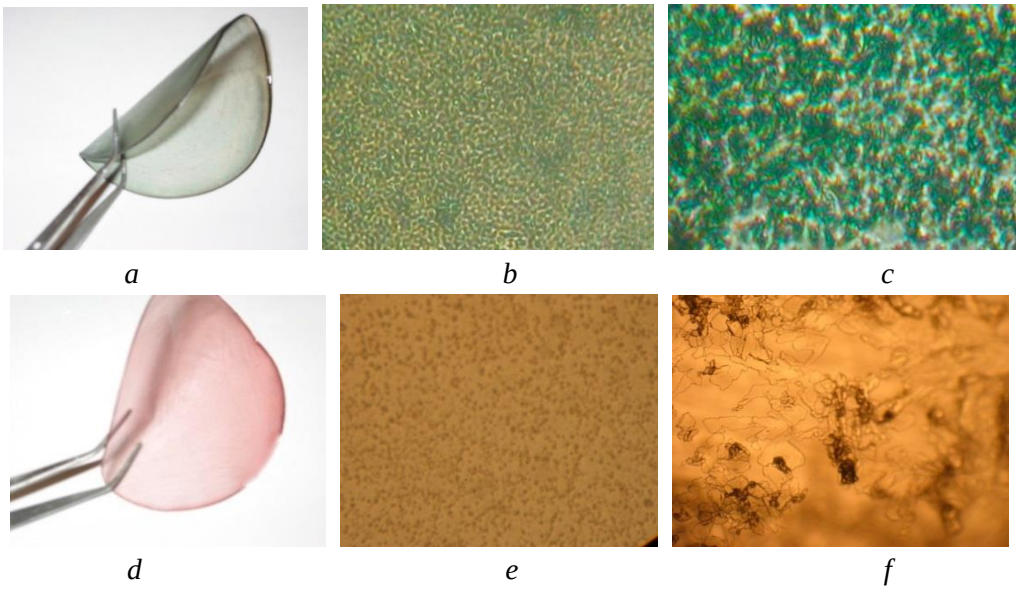

Figures 1.6 Microphotographs of composite polymer films: PVA-PoT (*a*, *b*), PVA-PAn (*c*), PMAA-PoA (*d*, *e*), PAA-PoT (*f*). Zoom 600 (*b*, *c*, *e*, *f*).

Film composites of polyaminoarenes in highly elastic polymer matrices under the influence of polar gases (ammonia) exhibit a gas-chromic effect with general laws similar to those observed for films of individual polyaminoarenes [49]. There is a significant change in the optical absorption spectra of composites under the action of ammonia. The general increase of intensity (Fig. 1.7, *a*, *b*) and shift of the position of the maxima of absorption bands (Fig. 1.7, *b*) are observed. The most significant changes were found for the band at 750–830 nm (absorption in the polaron zone) for PVA-PAn films. The action of ammonia caused almost complete neglect of this band due to the deprotonation processes with the formation of ammonium cations and the decrease of the carrier's concentration. Instead, a band appears at 580–620 nm, attributed to the imino-quinone fragments in the structure of polyaminoarenes [66, 67].

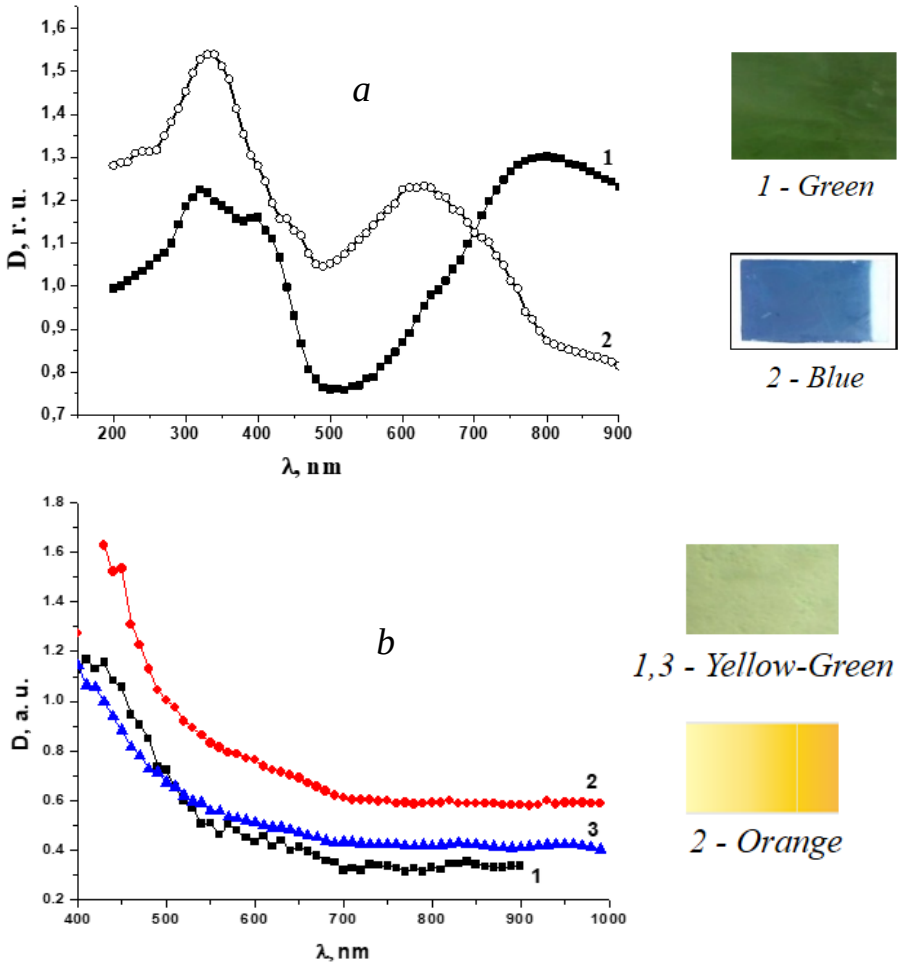

Figure 1.7 (*a*) Absorption spectra of composite films PVA-PAn (7.2 w. %) on air (*1*) and in ammonia environment, P = 1.4 kPa (*2*). The thickness of the film is 0.15 mm. (*b*) Absorption spectra of PVA-PoA (8,0 w. %) films on air (*1*), in ammonia environment (*2*), and after resorption in the air for 2 h (*3*). The thickness of the film is 0.12 mm.

Importantly visual changes in the color of the film are observed simultaneously. At the initial moment, the PVA-PAn film has an intense green color and retains it in the absence of ammonia in the media, indicating the freshness of the food product. The color of the indicator changes from green to blue in the presence of small amounts of ammonia (partial pressure P = 10–30 Pa). Production of films based on PAn derivatives, for example, PoT or PoA allows for a significant expansion in the color set. Because of food freshness losses, the color of the indicator changes dramatically - from bright green to blue for PAn and PoT or from yellow-green to orange for PoA. The allocation of ammonia is intensified if the food product is spoiled. Accordingly, the sensory film becomes pale blue for PAn and PoT or burgundy for PoA

The response speed of the sensor based on polymer composites depends on the temperature, gas pressure, and type of indicator substance embedded in the polymer matrix, but generally ranges from a few seconds to several minutes.

For practical realization, we offer available flexible indicator films based on the composites of elastic polymer matrices (PVA, PAA, PMAA) with conjugated polyaminoarenes, changing their color under the action of gases. The polymer matrices do not affect the regularities of optical absorption, ensuring the use of synthesized composites for gas sensor production.

1.3 Nanofabrication of Hybrid Structures Semiconductor – Conjugated Polymer

Improving the efficiency of organic electronic devices is possible due to the development of hybrid nanocomposites based on conducting polymers with dielectric matrices or inorganic semiconductors. These composites ccan be fabricated by simple, safe, and energy-saved methods without vacuum technologies. Semiconductor materials with spatially inhomogeneous structures, layered, porous, or dispersive, attract special attention due to the possibility of a new type of hybrid materials formation [68–72].

The methods of obtaining nanostructures based on polymers and semiconductors have attracted great attention due to the prospect of solar cells, light-emitting diodes, sensors, lasers, and memory device production [72–75]. Especially, the heterogeneous systems based on nano-crystal porous silicon (pSi) have a wide application in optoelectronics and sensor devices. The luminescence in the visible and near IR regions of the spectrum is one of the most important properties of such structures. The excitation of luminescence is possible due to the quantum-size effects as a result of the porous structure nanometer size [76]. Heterostructures based on pSi and surface organic layers, namely, conjugated conducting polymers, have been studied intensively [75, 77].

Heterogeneous systems based on nanostructured organic and inorganic semiconductors can be considered a new class of hybrid materials with enhanced functionality. A polymer film on the surface of a semiconductor can serve as a protective layer or create an electrical contact, thereby influencing the spectra of photosensitivity, absorption or emissi-

on, and electro-optical and sensory characteristics of nanostructures. We studied the physiccal and chemical processes occurring under the conditions of formation of conjugated polymers in nanostructured semiconductor media: porous silicon (pSi) [73–75], layered crystals of GaSe, InSe [78, 79], nanostructured TiO_2 [80], etc., structure and properties of the obtained nanomaterials. To identify the regularities of the interaction of components in polymer-semiconductor hybrid nanosystems, a complex approach was applied, namely, the study of the structure, chemical composition, and surface morphology of nanostructured semiconductors and organic-inorganic composites by electron and atomic force microscopy, X-ray diffraction, and IR spectroscopy. The effect of surface modification of nanostructured semiconductors on the radiation spectra characteristics, changes in electrical and optical characteristics, and sensor sensitivity were evaluated.

1.3.1 Formation of Hybrid Nanostructures Based on Porous Silicon

The electronic properties of silicon can be changed due to the formation of nanostructures – spatially separated silicon areas with minimum dimensions of several nanometers. In this case, the charge carriers acquire additional energy due to the quantum effect [72].

Among the techniques for obtaining silicon-based nanostructures, the most accessible is the creation of nanocrystals by etching voids with dimensions of several nanometers in single-crystal silicon. This material, called porous silicon, has the light-emitting ability and other unique properties that make it a valuable material for the production of sensors. The photoelectrochemical etching was used to obtain pSi, covered in works [74, 75].

To clarify the nature of the surface formations, the topology of the obtained pSi was investigated by atomic force microscopy (AFM). It was established that with fairly high homogeneity of the polished surface of the single crystal, there are certain surface defects. These protrusions, up to 2 nm high, can be centers for the structural inhomogeneities formation during the anodization of the sample (Fig. 1.8).

A comparison of AFM images of the surface of monocrystalline silicon before and after etching indicates the periodic structural modifications that can be attributed to the pSi layer. The pSi surface after anodization has vertical cylindrical protrusions, formed because of electrochemical etching of separate areas on the monocrystalline silicon surface (Fig. 1.8, *b*). By profile analysis of AFM images, it was determined that the depth of protrusions in the pSi reaches 45–50 nm with a total thickness of the etched layer of about 5 μm.

The chemical composition of the surface was identified by FTIR spectroscopy (Fig. 1.9, *a, b*). For monocrystalline silicon, an absorption band at 1100 cm^{-1}, corresponding to Si-O-Si valence vibrations [81], and at 620 cm^{-1}, corresponding to the deformation mode of $Si-H_2$ [82], were found. The absorption band at 1100 cm^{-1} is caused by silicon oxidation, and at 620 cm^{-1} – by water molecules adsorbed from the air.

The IR spectrum of pSi revealed an absorption band at 1100 cm^{-1}, observed in mono-Si (Si-O-Si oscillations), as well as oscillations of the C-O bond, corresponding to an absorption band at 1111 cm^{-1}, C-C oscillations at 1188 cm^{-1}, CH_2-OH, CH-OH and C-OH

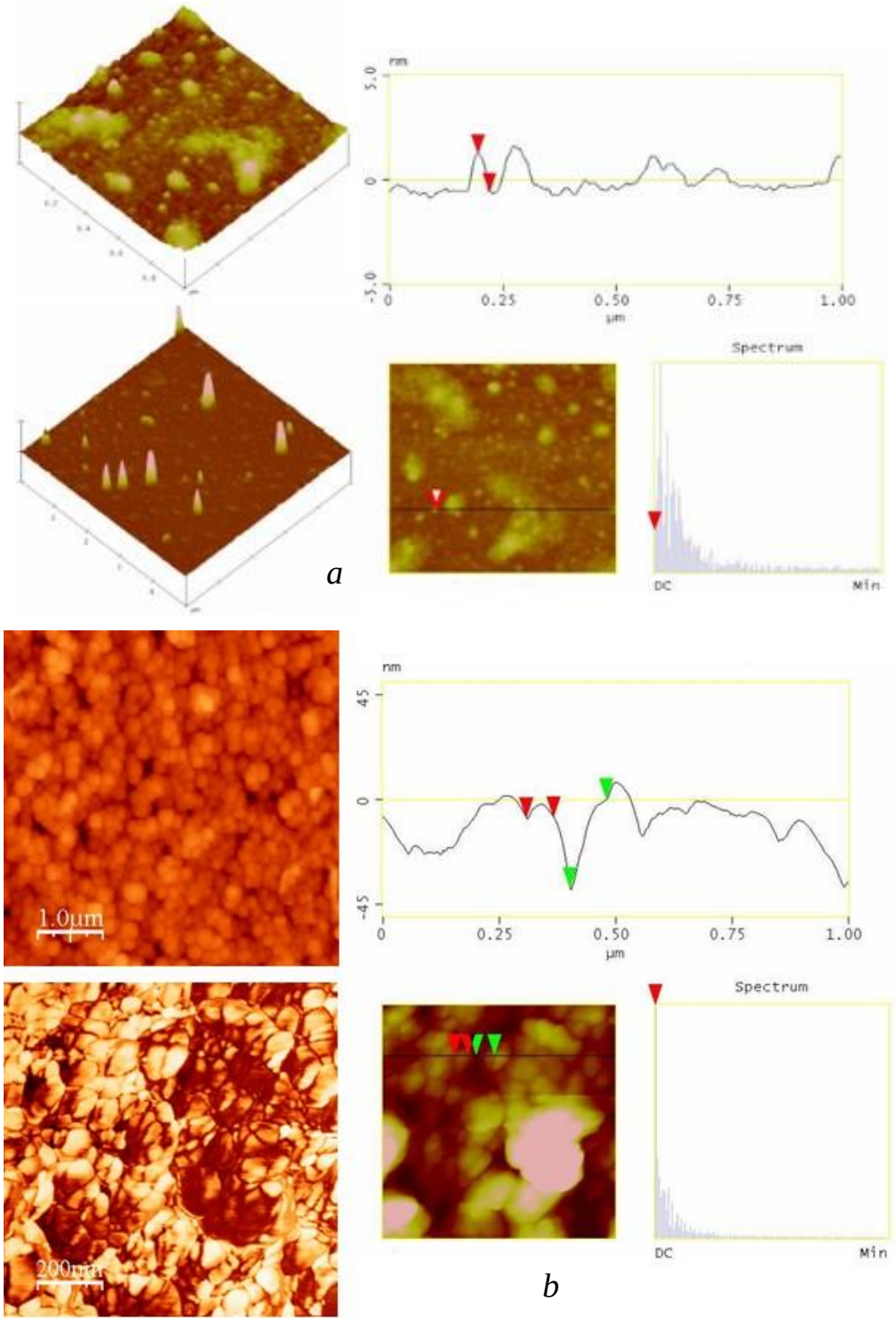

Figure 1.8 AFM image and surface profile of porous silicon before (*a*) and after (*b*) photoelectrochemical etching

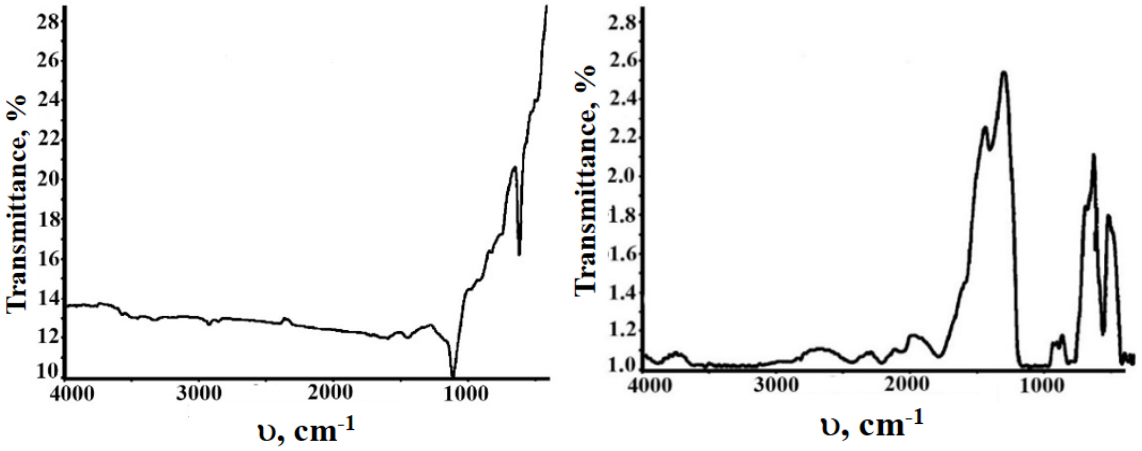

a *b*

Figure 1.9 FTIR transmission spectra of single crystal silicon (*a*) and porous silicon (*b*)

vibrations at 1050, 1072, and 1097 cm^{-1}, respectively, and Si-O-Si vibrations at 1240 cm^{-1}. The broad absorption band at 2900–3620 cm^{-1} corresponds to the absorption of O-H bond vibrations in water molecules adsorbed on the pSi surface [45, 46]. The absorption band at 835–890 cm^{-1} is associated with the adsorption of water molecules and fluorine because of the etching of pSi in HF. Absorption bands at 940 and 980 cm^{-1} are associated with the vibration of hydrogen and hydroxyl groups.

Therefore, the newly formed developed surface of nanocrystalline silicon has a complex chemical structure. The presence of functional groups makes it very sensitive to external factors. Conjugated polymers, integrated into the pores of nanocrystalline silicon, can act as a passivating layer and cause new functional properties appearance.

Porous silicon-polymer nanostructures are obtained by electropolymerization in two ways – galvanostatic electrolysis of pSi in a monomer solution [77] or electrochemical etching of monocrystalline silicon in the presence of monomer in the etching solution. In the second case, electrochemical polymerization processes take place simultaneously with etching [78], and the thickness of the polymer layer is uncontrolled. At the same time, the anodic current densities used for silicon anodization (20–60 mA/cm^2) correspond to high positive potentials and lead to significant electrochemical degradation of the polymer. Therefore, an important condition is the control of electrochemical polymerization potentials. This possibility can be provided by electrochemical polymerization in the cyclic potential sweep mode [84].

For example, the polymerization of *o*-anisidine is evidenced by the gradual increase of the response currents on the cyclic voltammograms (CVA) (Fig. 1.10, *a*). The appearance of redox maxima, characteristic of an electroactive polymer, on the CVAs is evidence of the formation of a pSi-polymer heterostructure. The linear dependence of the current of the anode peak I_p at E = 0.4–0.6 V on the number of cycles of the potential sweep at N = 4–16 allows for controlling the thickness of the electroactive polymer films. It was established, the amount of charge (Q) and, accordingly, the mass of the polyarene, integrated into

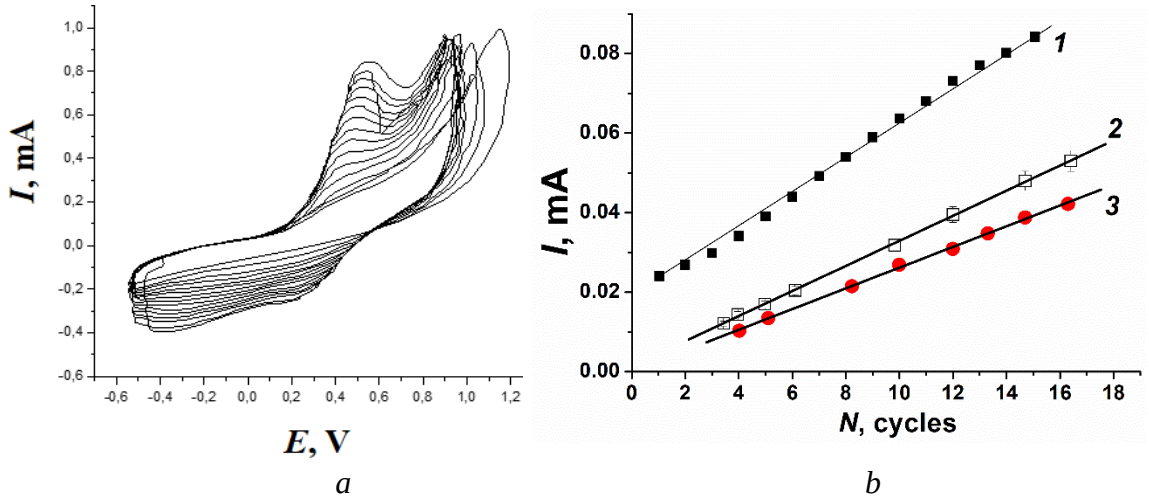

Figure 1.10 (*a*) CVA obtained during electrochemical polymerization of PoA on the pSi surface from 0.1 M solution of *ortho*-anisidine in 0.5 M H_2SO_4 at a potential scan rate of 40 mV/s; (*b*) Dependence of the current of the CVA anodic maximum on the number of cycles for obtaining pSi-PAn (*1*, *2*) and pSi-PoA (*3*) heterostructures. Potential scan rate: 80 (*1*) and 40 (*2*, *3*) mV/s.

the pSi, depends on the speed (ν) and the number of scanning cycles (*N*) of the potential during electrochemical polymerization. At a constant ν the maximum currents change proportionally to *N* in the process of formation of conducting polymer on the pSi surface (Fig. 1.10, *b*). According to the statistical analysis of AFM images of the pSi surface and obtained nanostructures (Fig. 1.11) the thickness of the pSi-polymer hybrid layer reaches 40–45 nm with a pSi pore depth of more than 200 nm. While the globular structure of the polymer is preserved.

The value of the cubic cell parameter "*a*" found from the X-ray diffraction data for pSi samples is 5.42467 Å, and for the pSi-PAn is 5.42984 Å. The error of the experiment did not exceed 10^{-3}Å, so it can be assumed some growth of the parameter *a* and, accordingly, the volume of the unit cell due to the formation of PAn chains in the pores of silicon.

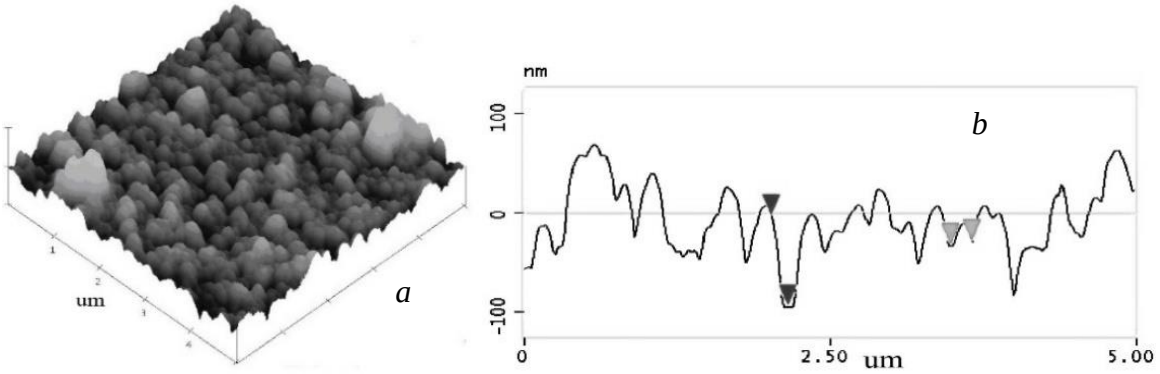

Figure 1.11 AFM image (*a*) and profile analysis (*b*) of the porous silicon surface with PAn film

Obtained pSi-polymer samples were studied for photo- (cathode) luminescence and sensor sensitivity [73–75, 85]. The newest approach to the formation of polymer-semiconductor hybrid nanostructures is the creation of electrochromic systems with optical properties controlled by applying voltage or current.

1.3.2 Electrochromic Structures Based on Porous Silicon and Polymer

Porous silicon nanostructures have a wide band of visible PL [74] allowing to change the intensity and spectral position of the emission maximum within wide limits with optical filters, in particular electrochromic polymer films. The transmission spectra of such films can be changed by applying an electric current. In addition, a silicon plate with a porous layer is not only a substrate for the electrochemical polymerization of PAn but also an electrode of an electrochromic cell [86, 87].

The PAn thin-film coating is transparent to both excitation and pSi-generated radiation. An important property of conjugated polymers is the ability to change electrical and optical characteristics depending on the degrees of oxidation [88]. The electrochromic effect of PAn films can be used in organic displays, shutter and filter optical devices, and optical sensors [88, 89]. It is possible to control the PL spectrum of nanoporous silicon by the color change and color intensity of PAn films under the applied voltage. We proposed a hybrid nanostructure for the production of fluorescent devices with an electrically controlled emission band [87].

The external voltage applied to the electrochromic structure causes a change in the optical transmittance of PAn film at 600–750 nm and, respectively, a change in the radiation intensity in the long-wavelength part of the PL spectrum of pSi. The change of voltage from –10 to +10 V causes the change of spectral maximum from 635 to 600 nm and a decrease in PL intensity (Fig. 1.12, 1.13).

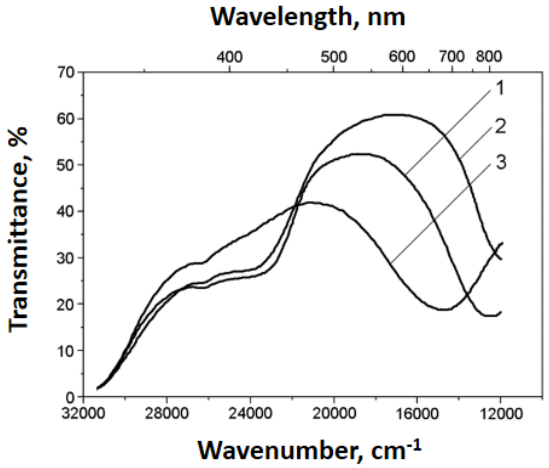

Figure 1.12 PL spectra of an electrochromic structure based on pSi (*1*) with an applied voltage of 10 V (*2*) and +10 V (*3*)

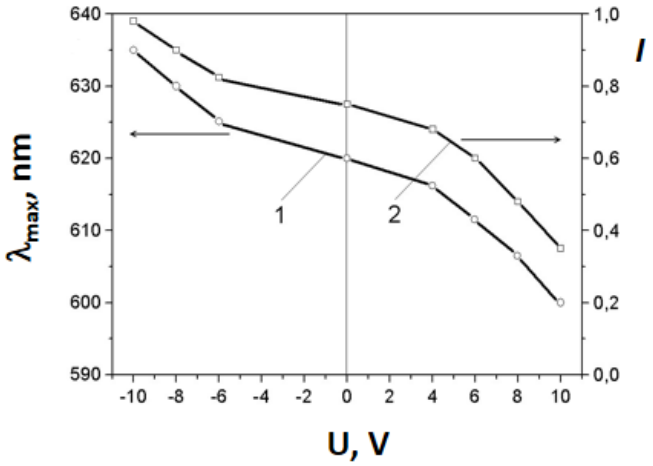

Figure 1.13 Dependence of the spectral position of the PL maximum (*1*) and its integral intensity (*2*) on the voltage applied to the electrochromic structure

The optical transmittance spectra of the PAn film depend on the magnitude and polarity of the applied voltage, due to the processes of electron and proton transport with the transformation of various forms of the polymer [88]. PAn changes from the colorless reduced state (leucoemeraldine), which transmits light in the entire visible part of the spectrum, to the green semi-oxidized form (emeraldine salt), which absorbs light in the wavelength range of 500–650 nm. Completely oxidized polyaniline (pernigraniline) is dark blue, almost black, and absorbs light in almost the entire visible range of the spectrum. Therefore, because of the electrochromic effect, the PAn film can reversibly change its color from almost transparent to yellow, green, and blue and transitional shades with a corresponding change in optical spectra.

The change in the optical properties of polyaniline in the SnO_2-PAn-pSi-Si hybrid structure has a similar nature to electrochromic effects in proton electrolytes. It is caused by changes in the oxidation degree of the CP under an external potential. The use of PAn as an active electrochromic layer opens up the possibility of creating optical elements operating according to the two-electrode scheme. Thus, PAn films deposited on the surface of porous silicon can act as an optical filter of pSi photoluminescence radiation with an electrically controlled transmission band.

1.3.3 "In situ" Fabrication of Hybrid Nanostructure with Layered Semiconductors

Two-dimensional (2D) semiconductor nanocrystals fabricated in the platelike form have been intensely investigated since the invention of single-layer graphene. GaSe with chemically passive selenium terminated surfaces is among the desirable materials for the production of single-layers 2D plates, even extracted and isolated from bulk. Several

groups succeeded in mechanical [90, 91], thermal, and laser-induced [92] GaSe exfoliation. Recent perspective [93] indicates that 2D platelike nanoparticles (including GaSe) are excellent PL emitters due to suppression of the absorption strengths into one electronic state contrary to the band for bulk material. Not far ago we found that the mutual interaction of components in the hybrid composites containing GaSe and conducting PAn leads to an essential conductivity increase, UV shifting in GaSe luminescence spectra, responsible for plate-like particle formation, etc [4].

Preparation of composite was carried out by oxidative polymerization of aniline under ammonium persulfate $(NH_4)_2S_2O_8$ in an aqueous medium in the presence of toluene sulfonic acid (TSA) as a doping and stabilizing agent. Method of obtaining composite consists of several stages. Originally performed dispersing a sample (45–150 mg of GaSe plates or nanopowder GaSe with particle size 60-80 nm) in a solution of surfactant – 0.12 M TSA using ultrasound for 30 min. Then 0.205 g of monomer droplets were injected in GaSe dispersion with continuous stirring, and after 10 min 0.005 ml of 0.47 M solution of oxidant $(NH_4)_2S_2O_8$ was added. The process was carried out at T = 293 K for 24 hours. Finally, a dark dispersion of composite was isolated in the form of the precipitate by centrifuging. For investigations, we took samples with the content of inorganic component 10–12 wt. % [94].

TEM images of PAn-powdered GaSe samples are presented in Fig. 1.14. Expanded images (Fig. 1.14, *a*, *b*) demonstrate the presence of two types of nanoobjects: thin stripes (up to few nanometres in height and up to 100 nm in length) and discs with rather broad diameters distribution (5–20 nm). As shown by HRTEM (Fig. 1.14, *c*, *d*) the heights of such stripes consist of GaSe elementary sandwiches, packed along *c* crystallographic axis. It should be noted; that there is an essential broadening of lattice plane spacing in this direction yielding 0.833 nm. Compared with the same value for bulk GaSe materials (0.796 nm for (0002) plane spacing), the *c* lattice parameter increased by about 4,4 %. The elementary tetralayers of GaSe structure along direction are somehow bent by mechanical stresses, applied normally to that direction on the whole particles (Fig. 1.14 *c*, *d*), but we did not observe any extended defects or elementary tetralayers fractures. The number of such monolayers (ML) per particle could vary in the 1020 range (5–10 lattice parameters). The smaller particles (1–2 ML) during interaction with electron beam collinear to edges in plate-like particle geometry simply do not effectively scatter electrons to make them visible by TEM, by were detected by optical measurements earlier [95] and as discs on Fig. 1.14, *a*, *e*. They are the same particles but the top/bottom of them are oriented normally to the electron beam. We can also observe lattice fringed on one well oriented with respect to electron beam particle: this time the spacing yields 0.969 nm coinciding exactly with a triple value of (10–10) lattice plane [96]. From TEM and HRTEM images we suggest that particles are a few ML thick to observe lattice spacing similar to mechanically exfoliated GaSe flakes [91].

Gallium monoselenide crystal lattice consists of tetralayers –Se–Ga–Ga–Se–, bounded by the week van der Waals forces. The distance between layers of Se-Se is approximately 3.25 Å. It is possible to include polymeric chains of PAn between layers of Se-Se (the width of an aniline molecule is about 2.5 Å at the thickest point of the benzene ring).

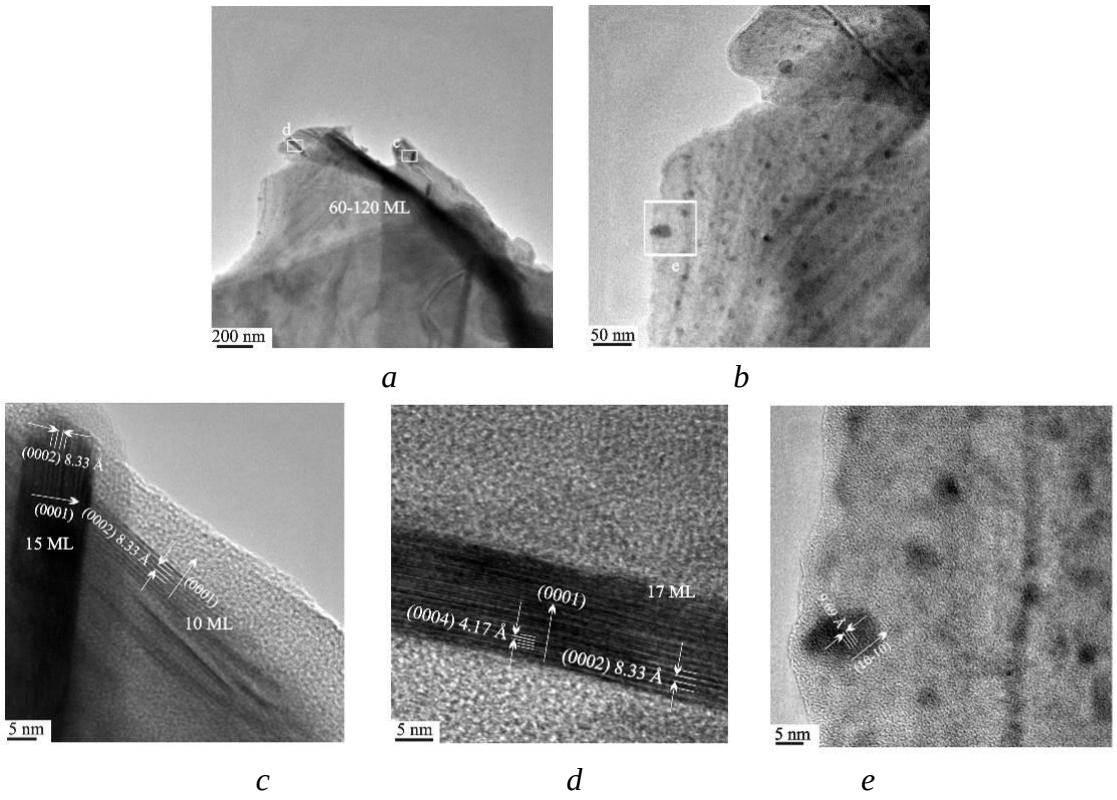

Figure 1.14 Representative (*a*, *b*) TEM and HRTEM (*c*, *d*, *e*) of boxed areas (in *a*, *b*) images of exfoliated by PANI GaSe nanoparticles. In the (*c*, *d*) images the lattice planes could be attributed to the (0001) direction along the crystallographic *c* axis, while in the (*e*) image – to the (10–10) direction along the crystallographic axis of hexagonal GaSe.

But polymerization obviously results in a much larger spatial hindrance of long PAn molecules when forming crystalline composite structures based on hexagonal GaSe. This changes the diffraction pattern [96], which now does not accurately describe the prevailing model of orientation, creating the additional diffraction reflections and clearly elucidated by HRTEM. When powdering the single crystal plates this composite phase is apparently saved, but there is simply hexagonal GaSe, in contrary to the sample PAn-GaSe. As was mentioned earlier [95], powdered fractured GaSe samples exhibit numerous extended defects-cleavage stairs on the surface. The aniline molecules diffuse into them during filling the van der Waals gap of particles with the further formation of a few ML composites based on PAn-GaSe. The model of such interaction is presented in Fig. 1.15.

The edges of GaSe tetralayer sandwiches have high adsorption activity. The terminal gallium atoms on the surface of the nanoparticles act as a strong Lewis acid. Amino groups, on the other hand, are Lewis bases, leading to the adsorption of aniline on defects. Adsorbed aniline molecules diffuse into the van der Waals gap (vdW9) with linear dimensions commensurate with the dimensions of the benzene ring. The polymerization of aniline leads to the formation of free tetralayer GaSe plates wrapped by polyaniline chains, ensuring

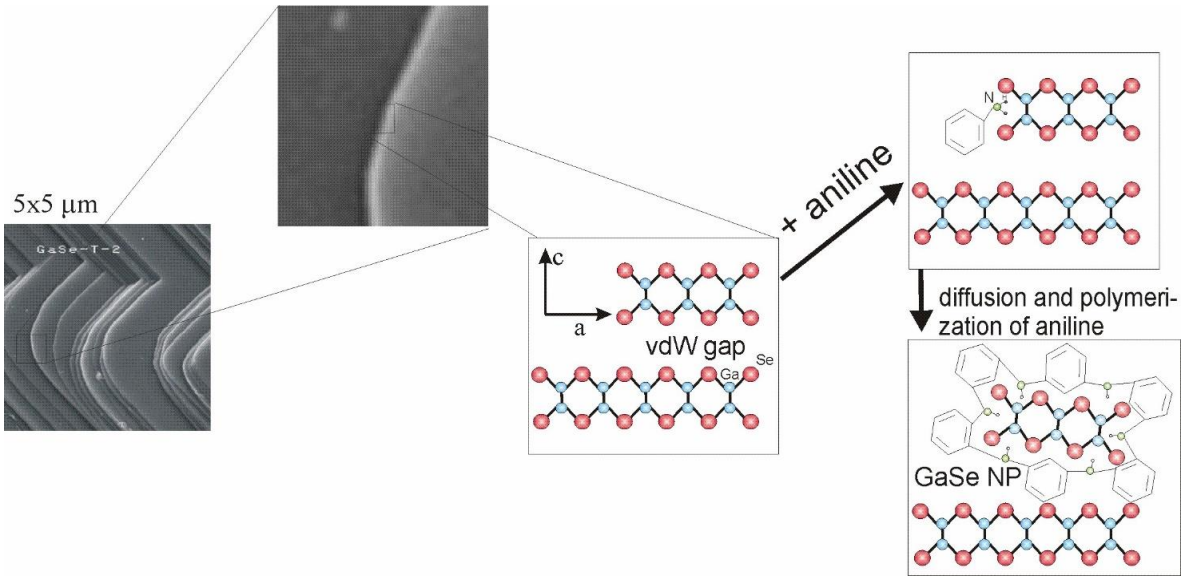

Figure 1.15 Schematic representation of the interaction of GaSe nanoparticles with polyaniline [94]

good gallium passivation at the ends of the plates. In this way, graphene-like particles stabilized by a polymer nanolayer are formed.

1.4 Conclusion

The methods of electrochemical and "in situ" polymerization are extremely promising for the synthesis of hybrid nanostructures based on conductive polymers and dielectric polymer matrices, as well as porous or layered semiconductor structures. Such materials are characterized by increased optical, sensory, and electrochromic activity. The improvement of the properties of the obtained nanomaterials is caused by the formation of conductive polymer chains directly in the dielectric polymer matrix or in the pores of the semiconductor. As a result, the characteristic nanometer dimensions of the hybrid structure and the electronic properties of the conjugated polymer are preserved.

Keywords

- polymerization
- conducting polymer
- dielectric matrix
- structure
- percolation
- porous silicon
- luminescence
- gas sensors

References

1. *Aguilar M. R., Román J. S.* Smart polymers and their applications. Second edition. Woodhead Publishing: Sawston, Cambridge, 2019. 687 p. DOI: https://doi.org/10.1016/C2017-0-00049-6
2. *Shahinpoor M., Schneider H.-J.* Intelligent Materials. RSC Publishing: London, 2007. 532 p. DOI: https://doi.org/10.1039/9781847558008
3. *Aksimentyeva O. I., Tsizh B. R., Horbenko Yu. Yu., Konopelnyk O. I., Martynyuk G. V., Chokhan' M. I.* Flexible elements of gas sensors based on conjugated polyaminoarenes // Mol. Cryst. Liq. Cryst. 2018. Vol. 670 (1). P. 3–10. DOI: https://doi.org/10.1080/15421406. 2018.1542057.
4. *Feron K., Lim R., Sherwood C., Keynes A., Brichta A., Dastoor P. C.* Organic bioelectronics: Materials and biocompatibility // J. Mol. Sci. 2018. Vol. 19 (8). DOI: https://doi.org/10.3390/ ijms19082382
5. *Heeger A. J.* Semiconducting and metallic polymers: the fourth generation of polymeric materials // Synth. Met. 2002. Vol. 123. P.23−42. DOI: https://doi.org/10.1021/jp011611w
6. *Aksimentyeva O. I., Konopelnyk O. I., Martyniuk G. V.* Synthesis and physical–chemical properties of composites of conjugated polyaminearenes with dielectric polymeric matrixes // Computational and Experimental Analysis of Functional Materials. Apple Academic Press: New York, 2017. P. 331−370. DOI: https://doi.org/10.1201/9781315366357
7. *Ziadan K. M., Hussein H. F., Ajeel K. I.* Study of the electrical characteristics of poly(o-toluidine) and application in solar cell / Energy Procedia. 2012. Vol. 18. P. 157–164. DOI: https://doi.org/ 10.1016/j.egypro.2012.05.027
8. *Khan A., Jawaid M., Khan A. A. P., Asiri A. M.* Electrically conductive polymers and polymer composites: from synthesis to biomedical applications. Wiley: Hoboken, New Jersey, 2018. 264 p.
9. *Bakhmatyuk B. P., Aksimentyeva O. I., Dupliak I. Ya., Horbenko Yu. Yu.* Electrochemical properties of polyaniline in aqueous environments of iodide and bromide in the system of electrochemical energy source // Phys. Chem. Solid State. 2016. Vol. 17 (2). P. 234–240. DOI: https://doi.org/ 10.15330/pcss.17.2.234-240. (in Ukrainian).
10. *Aksimentyeva O. I., Chepkov I. B., Filipsonov R. V., Malynych S. Z., Gamernyk R. V., Martyniuk G. V., Horbenko Yu. Yu.* Hybrid composites with the low reflection of IR radiation // Phys. Chem. Solid State. 2020. Vol. 21 (4). P. 764–770. DOI: https://doi.org/10.15330/ pcss.21.4.764-770
11. *Aksimentyeva O., Konopelnyk O., Olenych I., Poliovyi D., Horbenko Yu., Myhalets A.* Physical-chemistry of electro-optical phenomena in conjugated polymer systems Proceedings of the VI Ukrainian Congress of Electrochemistry, Lviv, Ukraine, 4-7 June 2018. P. 112–114. (in Ukrainian).
12. *Mac Diarmid A. G.* "Synthetic metals": a novel role for organic polymers (Nobel lecture) // Angew. Chem. Int. Ed. 2001. Vol. 125. P. 11–22. DOI: https://doi.org/10.1016/S0379-6779(01)00508-2
13. *Martynyuk G. V., Aksimentyeva O. I.* Features of charge transport in polymer composites polymer-thylmethacrylate – polyaniline // Phys. Chem. Solid State. 2020. Vol. 21 (2). P. 319–324. DOI: https://doi.org/10.15330/pcss.21.2.319-324.
14. *Aksimentyeva O., Konopelnyk O., Opaynych I., Tsizh B., Ukrainets A., Ulansky Y., Martyniuk G.* Interaction of components and conductivity in polyaniline-poly(methylmethacrylate) nanocomposites // Rev. Adv. Mater. Sci. 2010. Vol. 23 (2). P. 185–188.
15. *Aksimentyeva O. I.* Electrochemical methods of synthesis and conductivity of conjugated polymers. Svit: Lviv, 1998. 123 p. (in Ukrainian).
16. *Tarasevich Yu. Yu.* Percolation. Theory. Application. Algorithms. Chemistry: Moskow, 2002. – 110 p. (in Russian).
17. *Christensen K.* Percolation theory. MIT Press: London, 2002, 40 p.

18. *Mamunya E. P., Yurzhenko M. V., Lebedev E. V., Levchenko V. V., Chervakov O. V., Matkovska O. K., Sverdlikovska O. S.* Electroactive polymeric materials. Alpha Reklama: Kyiv, 2013. 402 p. (in Ukrainian).
19. *Herega A.* Some applications of the percolation theory: review of the century beginning // J. Mater. Sci. Eng. 2015. Vol. 5. P. 409–414 DOI: https://doi.org/10.17265/2161-6213/2015.11-12.004
20. *Lysenkov E. A., Klepko V. V.* Analysis of the percolation behavior of electrical conductivity of systems based on polymer and carbon nanotubes // Journal of *Nano*- and Electronic Physics. 2016. Vol. 8 (1).
21. *Zabrodsky A. G., Nemov S. A., Ravych Yu. I.* Electronic properties of disordered systems. Nauka: St. Petersburg, 2000. 72 p.
22. *Efros A. L., Shklovskii B. I.* Critical behaviour of conductivity and dielectric constant near the metal-non-metal transition threshold // Phys. Status Solidi. 1976. Vol. 76 (2). P. 475–485. DOI: https://doi.org/10.1002/pssb.2220760205
23. *Berezkin V. I., Popov V. V.* Percolation transition in carbon composites based on fullerenes and thermally expanded graphite // Phys. Solid State. 2018. Vol. 60 (1). P. 202–206. DOI: https:// doi.org/10.1134/S1063783418010043
24. *Yevchuk O., Aksimentyeva O., Horbenko Yu.* Optical and electrical properties of the conjugated polyaminoarenes composites with polymer electrolytes // Visnyk Lviv Univ., Ser. Chem. 2012. Vol. 53. P. 352–356. (in Ukrainian).
25. *Aksimentyeva O., Dutka V., Horbenko Yu., Martynyuk H., Riy U., Halechko H*. Composites of the conductive polyaminoarenes in the matrix of styromal // Proc. Shevchenko Sci. Soc. Chem. Sci. 2017. Vol. XLVIII. P. 7–16.
26. *Martyniuk G., Aksimentyeva O.* Influence of conductive polymer filler on electrical conductivity and microhardness of composites with dielectric polymeric matrices // Proc. Shevchenko Sci. Soc. Chem. Sci. 2020. Vol. LX. P. 14–21. DOI: https://doi.org/10.37827/ntsh.chem. 2020.60.014
27. *Berëzkyn V. Y., Popov V. V.* Percolation transition in carbon composite on the basis of fullerenes and exfoliated graphite // Phys. Solid State. 2018. Vol. 60 (1). P. 207–211. DOI: https://doi.org/ 10.1134/S1063783418010043
28. *Eletskyi A. V., Knyzhnyk A. A., Potapkyn B. V., Kenny Kh. M.* Influence of methods of formation of polymer composite materials with carbon nanotubes on mechanisms of electrical conductivity // UFN. 2015. Vol. 185, 225. DOI: https://doi.org/10.3367/UFNr.0185.201503a.0225 (in Russian).
29. *Afanasov Y. M., Morozov V. A., Seleznev A. N., Avdeev V. V.* Conductive composites on the basis of thermally expanded graphite // Inorg. Mater. 2008. Vol. 44 (6).
30. *Aksimentyeva O. I., Martyniuk G. V.* Percolation phenomena in the polymer composites with conducting polymer fillers // Phys. Chem. Solid State. 2021. Vol. 22 (4). P. 811–816. DOI: https:// doi.org/10.15330/pcss.22.4.811-816
31. *Kahol P. K., Ho J. C., Chen Y. Y., Wang C. R., Neeleshwar S., Tsai B., Wessling C.* On metallic characteristics in some conducting polymers // Synth. Metals. 2005. Vol. 151 (1). P. 65–72. DOI: https://doi.org/10.1016/j.synthmet.2005.03.017
32. *Shaari H. A. H., Ramli M. M., Mohtar M. N., Rahman N. A., Ahmad A.* Synthesis and conductivity studies of poly(methyl methacrylate) (PMMA) by co-polymerization and blending with polyaniline (PANi) // Polymer. 2021. Vol. 13 (12). DOI: https://doi.org/10.3390/ polym13121939
33. *Adhikary S., Banerji P.* Polyaniline composite by in situ polymerization on a swollen PVA gel // Synth. Met. 2009. Vol. 159. P. 2519–2524. DOI: https://doi.org/10.1016/j.synthmet. 2009.08.050
34. *Lapkowski M., Geniès E. M.* Evidence of two kinds of spin in polyaniline from in situ EPR and electrochemistry: Influence of the electrolyte composition // J. Electroanal. Chem. Interfacial Electrochem. 1990. Vol. 279 (1-2). P. 157–168. DOI: https://doi.org/10.1016/0022-0728(90)85173-3.

35. *Srinivasan D., Natarajan T. S., Bhat S. V., Wessling B.* Electron spin resonance absorption in organic metal polyaniline and its blend with PMMA // Solid State Commun. 1999. Vol. 2 (5). P. 503–508. DOI: https://doi.org/10.1016/S0038-1098(99)00109-X
36. *Al-Thani, N., Hassan, M. K., Bhadra, J.* Polyaniline/polystyrene blends: in-depth analysis of the effect of sulfonic acid dopant concentration on ac conductivity using broadband dielectric spectroscopy // Int. J. Polym. Sci. 2018. Vol. 2018. DOI: https://doi.org/10.1155/2018/ 1416531
37. *Manoharan D., Chandrasekaran J., Maruthamuthu S., Kathirvel P., Jayamurugan P.* Synthesis of poly(aniline-co-*o*-toluidine) nanocolloidal particles in aqueous poly(styrene sulfonic acid) by dispersion polymerization method // J. Nanostructure Chem. 2015 Vol. *5* (1). P. 115–122. DOI: https://doi.org/10.1007/s40097-014-0142-x
38. *Bhadra J., Al-Thani N. J., Madi N. K., Al-Maadeed M. A.* Preparation and characterization of chemically synthesized polyaniline - polystyrene blends as a carbon dioxide gas sensor // Synth. Met. 2013. Vol. 181. P. 27–36. DOI: https://doi.org/10.1016/j.synthmet.2013.07.026
39. *Bhadra J., Al-Thani N. J., Madi N. K., Al-Maadeed M. A.* High performance sulfonic acid doped polyaniline–polystyrene blend ammonia gas sensors // J. Mater. Sci. Mater. Electron. 2016. Vol. 27. P. 8206–8216. DOI: https://doi.org/10.1007/s10854-016-4825-6
40. *Schettini A. R. A., Soares B. G.* Study of microwave absorbing properties of polyaniline/STF conducting composite prepared by in situ polymerization // Macromol. Symp. 2011. Vol. 299–300. P. 164–174. DOI: https://doi.org/10.1002/masy.200900106
41. *Roichman Y., Titelman G. I., Silverstein M. S.* Polyaniline synthesis: influence of powder morphology on conductivity of solution cast blends with polystyrene // Synth. Met. 1999. Vol. 98. P. 201–209. DOI: https://doi.org/10.1016/S0379-6779(98)00190-8
42. *Kim Y. H., Park B. J., Choi H. J., Choi S. B.* Preparation of polystyrene/polyaniline composite particles and their electrorheology // J. Phys. Conf. Ser. 2009. Vol. 149. DOI: https://doi.org/ 10.1088/1742-6596/149/1/012017
43. *Ghasemi H., Sundarara U.* Electrical properties of in situ polymerized polystyrene/polyaniline composites: The effect of feeding ratio // Synth. Met. 2012. Vol. 162 (13–14). P. 1177–1183. DOI: https://doi.org/10.1016/j.synthmet.2012.04.037
44. *Sudha J. D., Sivakala S.* Conducting polystyrene/polyaniline blend through template-assisted emulsion polymerization // Colloid Polym. Sci. 2009. Vol. 287 (11). P. 1347–1354. DOI: https://doi.org/ 10.1007/s00396-009-2101-5
45. *Aksimentyeva O. I., Konopelnyk O. I., Horbenko Yu. Yu., Martyniuk G. V.* Nanofabrication of conducting polymerfillers in polymer matrix: Polystyrene-poly-o-toluidine composites // Mol. Cryst. Liq. Cryst. 2022. https://doi.org/10.1080/15421406.2022.2073531
46. *Stepura A. L., Aksimentyeva O. I., Demchenko P. Yu.* Features of the structure and physical-chemical properties of poly-ortho-toluidine doped with toluenesulfonic acid // Phys. Chem. Solid St. 2019. Vol. 20 (1). P. 77–82. DOI: https://doi.org/10.15330/pcss.20.1.82
47. *Khan A. A., Shaheen S.* Electrical conductivity, isothermal stability and amine sensing studies of a synthetic poly-o-toluidine/multiwalled carbon nanotube/Sn(IV) tungstate composite ion exchanger doped with p-toluenesulfonic acid // Anal. Methods. 2015. Vol. 7. P. 2077–2086. DOI: https:// doi.org/10.1039/C4AY02911A
48. *Qi X-Y., Yan D., Jiang Z., Cao Y-K., Yu Z-Z., Yavari F., Koratkar N.* Enhanced electrical conductivity in polystyrene nanocomposites at ultra-low graphene content // ACS Appl. Mater. Interfaces. 2011. Vol. 3 (8). P. 3130–3133. DOI: https://doi.org/10.1021/am200628c
49. *Aksimentieva O. I., Tsizh B. R., Chokhan M. I.* Sensors for control of gaseous media in the food industry and the environment: a monograph. Pyramida: Lviv, 2017. 284 p. (in Ukrainian).
50. *Kuswandi B.* Freshness sensors for food packaging. Reference module in food science. Elsevier, 2017. DOI: https://doi.org/10.1016/B978-0-08-100596-5.21876-3

51. *Dong X., Zhang X., Wu X., Cui H., Chen D.* Investigation of gas-sensing property of acid-deposited polyaniline thin-film sensors for detecting H_2S and SO_2 // Sensors. 2016. Vol. 16. P. 1888–2003. DOI: https://doi.org/10.3390/s16111889
52. *Horbenko Yu., Tsizh B., Dzeryn M., Olenych I., Aksimentyeva O., Bogatyrev V.* Sensitive elements of gas sensors based on poly-o-toluidine/silica nanoparticles composite // Acta Phys. Pol. 2022. Vol. 141 (4). P. 386–389. Doi: http://doi.org/10.12693/APhysPolA.141.386
53. *Shahzad N., Khalid U., Iqbal A., Rahman M. Ur.* eFresh – a device to detect food freshness // Int. J. Soft Comput. Eng. 2018. Vol. 8 (3). P. 1–4.
54. *Aksimentyeva O. I., Tsizh B. R., Horbenko Yu. Yu., Martyniuk G. V., Konopelnyk O. I., Chokhan' M. I.* Flexible elements of gas sensors based on conjugated polyaminoarenes // Mol. Cryst. Liq. Cryst. 2018. Vol. 670 (1). P. 3–10. DOI: https://doi.org/10.1080/15421406.2018. 1542057
55. *Park S. J. Park C. S., Yoon H.* Chemo-electrical gas sensors based on conducting polymer hybrids. Polymers. 2017. Vol. 9 (5). DOI: https://doi.org/10.3390/polym9050155
56. *Pandey S.* Highly sensitive and selective chemiresistor gas/vapor sensors based on polyaniline nanocomposite: A comprehensive review // J. Sci. Adv. Mater. Dev. 2016. Vol. 1. P. 431–453. DOI: https://doi.org/10.1016/j.jsamd.2016.10.005
57. *Mustafa F., Andreescu S.* Chemical and biological sensors for food-quality monitoring and smart packaging // Foods. 2018. Vol. 7. DOI: https://doi.org/10.3390/foods7100168
58. *Tsizh B. R., Chokhan M. I., Aksimentyeva O. I., Konopelnyk O. I., Poliovyi D. O*. Sensors based on conducting polyaminoarenes to control the animal food freshness // Mol. Cryst. Liq. Cryst. 2008. Vol. 497. P. 586–592. DOI: https://doi.org/10.1080/15421400802463043
59. *Tsizh B., Aksimentyeva O., Goliaka P., Chokhan M.* Gas sensors for analysis of food products. SPOLOM: Lviv, 2021. 236 p.
60. *Aksimentyeva O. I., Tsizh B. R., Horbenko Yu. Yu., Stepura A. L.* Detection of the organic solvent vapors by the optical gas sensors based on polyaminoarenes // Scientific Messenger of LNU VMB. Series: Food Technologies. 2021. Vol. 23 (95). P. 20–24. DOI: https://doi.org/ 10.32718/nvlvet-f9504
61. *Nynaru V., Jayamani E., Srinivasulu M., Han E. C. W., Bakri M. K. B* Short review on conductive polymer composites as functional materials // Key Eng. Mater. 2019. Vol. 796. P. 17–21. DOI: https://doi.org/10.4028/www.scientific.net/KEM.796.17
62. *Grosh M., Arman A., De S. K., Chatterjee S.* Low temperature electrical conductivity of polyaniline-polyvinyl alcohol blends // Solid State Commun. 1997. Vol. 103 (11). P.629–633. DOI: https://doi.org/10.1016/S0038-1098(97)00236-6
63. *Aksimentyeva O. I., Konopelnyk O. I., Tsizh B. R., Yevchuk O. M., Chokhan M. I.* Flexible elements of optical sensors based on conjugate polymer systems // SEMST. 2011. Vol. 2 (8). P. 34–39. (in Ukrainian).
64. *Aksimentyeva O. I., Ukrainets A. M., Konopelnyk O. I., Yevchuk O. M.* Method of obtaining conductive polymer composites. Patent № 53159 (UA). Publ.15.01.2003, Bull. №1. (in Ukrainian).
65. *Akimentyeva O. I., Tsizh B. R., Chokhan M. I., Yevchuk O. M.* Sensor for visual control of ammonia content. Patent № 65401 (UA). Publ. 12.12.2011, Bull. №23 (in Ukrainian).
66. *Sverdlova O.V.* Electronic spectra in organic chemistry. Khimiya: Leningrad, 1985. 248 p. (in Russian)
67. *Murrell I. N.* The theory of the electronic spectra of organic molecules // J. Chem. Educ. 1965. Vol. 42 (1). P. A58. DOI: https://doi.org/10.1021/ed042pA58
68. *Jung J., Chang M., Yoon H.* Interface engineering strategies for fabricating nanocrystal-based organic-inorganic nanocomposites // Appl. Sci. 2018. Vol. 8 (8). DOI: https://doi.org/10.3390/ app8081376
69. *Reddy K. R., Hemavathi B., Balakrishna G. R., Raghu A. V., Naveen S., Shankar M. V.* Organic conjugated polymer-based functional nanohybrids: Synthesis methods, mechanisms and its appli-

cations in electrochemical energy storage supercapacitors and solar cells // Polymer composites with functionalized nanoparticles. 2018. P. 357–379. DOI: https://doi.org/10.1016/B978-0-12-814064-2.00011-1

70. *Liu P.* Preparation and characterization of conducting polyaniline/silica nanosheet composites // Curr. Opin. Solid State Mater. Sci. 2008. Vol. 12. P. 9–13. DOI: https://doi.org/10.1016/j.cossms.2009.01.001
71. *Olenych I. B., Aksimentyeva O. I., Monastyrskii L. S., Dzendzeliuk O. S.* Effect of radiation on the electrical and luminescent properties of conjugated polymer–porous silicon composite // Mol. Cryst. Liq. Cryst. 2016. Vol. 640 (1). P. 165–172. DOI: http://doi.org/10.1080/15421406.2016.1257328
72. *Bisi O., Ossicini S., Pavesi L.* Porous silicon: a quantum sponge structure for silicon-based optoelectronics. Surface science reports // Surf. Sci. Rep. 2000. Vol. 38. P. 1–126. DOI: https://doi.org/10.1016/S0167-5729(99)00012-6
73. *Olenych I. B., Aksimentyeva O. I.* Photosensitive organic-inorganic hybrid structures based on porous silicon // Mol. Cryst. Liq. Cryst. 2018. – Vol. 671 (1). P. 90–96. DOI: https://doi.org/10.1080/15421406.2018.1542091
74. *Olenych I. B., Monastyrskii L. S., Aksimentyeva O. I., ed. Sattler K. D.* Chapter 22. Photovoltaic structures based on porous silicon // Silicon Nanomaterials Sourcebook: Arrays, Functional Materials, Industrial Nanosilicon. Volume two. CRC Press: USA, University of Hawaii at Manoa, 2017. P. 495**–**518. DOI: https://doi.org/10.4324/9781315153551
75. *Aksimentyeva O. I., Monastyrsky L. S., Savchyn V. P., Stakhira P. Y., Yarytska L. I., Pavlyk M. R.* Structure and luminescence properties of the hybrid composites: Porous silicon – polyphenylacetylene // Physics and Chemistry of Solis State. 2010. Vol. 11 (3). P. 690–695.
76. *Koyama H., Koshida N.* Electrical properties of luminescent porous silicon // J. Lumin. 1993. Vol. 57. P. 293**–**299. DOI: https://doi.org/10.1016/0022-2313(93)90147-F
77. *Halliday D. P., Eggleston J. M., Adams P. N., Pentland I. A., Monkman A. P.* Visible electroluminescence from polyaniline – porouse silicon junction // Synth. Met. 1997. Vol. 85. P. 1245–1246. DOI: https://doi.org/10.1016/S0379-6779(97)80223-8
78. *Voitovych S. A., Grygorchak I. I., Aksimentyeva O. I.* Lateral semiconductive and polymer conductive nano layered structures: preparing, properties and applying // Mol. Cryst. Liq. Cryst. 2008. Vol. 497. P. 55–54. DOI: https://doi.org/10.1080/15421400802458498
79. *Stakhira P. Y., Aksimentyeva O. I., Dorosh O. B., Savchyn V. P., Cherpak V. V., Konopelnyk O. I.* Properties of heterojunctions based on inorganic and organic semiconductors: Polyphenylacetylene-InSe(:Ag) heterostructure // Ukr. J. Phys. 2004. Vol. 49 (11). P. 1193–1198.
80. *Aksimentyeva O. I., Poliovyi D. O., Fechan A. V., Yevchuk O. M.* Nanostructured electrochromic layers // Mol. Cryst. Liq. Cryst. 2008. Vol. 497. P. 362–369. DOI: https://doi.org/10.1080/15421400802458225
81. *Tarutina L. I., Pozdniakova F. Yu.* Spectral analysis of polymers. Khimia: Leningrad, 1986. 248 p.
82. *Kopylov A. A., Holodilov A. N.* Infrared absorption in porous silicon obtained in electrolytes containing ethanol // Physics and Technics of Semiconductors. 1997. Vol. 31 (5). P. 470–472.
83. *Canham L. T.* Silicon quantum wire array fabrication by electrochemical and chemical dissolution of wafers // Appl. Phys. Lett. 1990. Vol. 57. P. 1046–1048. DOI: https://doi.org/10.1063/1.103561
84. *Aksimentyeva O. I., Monastyrsky L. S., Yevchuk O. M., Olenych I. B., Pavlyk M. R.* The method of obtaining polymer-semiconductor hybrid composites. Patent № 55629 (UA). Publ. 27.12.2010. Bull. №24. (in Ukrainian).
85. *Olenych I., Aksimentyeva O., Horbenko Y., Tsizh B.* Organic-inorganic nanocomposites for gas sensing // International Conference Radio Electronics & Info Communications (UkrMiCo), 2016. P. 1–3. DOI: https://doi.org/10.1109/UkrMiCo.2016.7739609

86. *Olenych I. B., Aksimentyeva O. I., Monastyrskii L. S., Pavlyk M. R.* Electrochromic effect in photoluminescent porous silicon – polyaniline hybrid structures // J. Appl. Spectrosc. 2012. Vol. 79 (3). P. 495–498. DOI: https://doi.org/10.1007/s10812-012-9629-8
87. *Olenych I. B., Aksimentyeva O. I., Monastyrskii L. S.* A method of obtaining an electrochromic structure based on porous silicon. Patent № 127257 (UA). Publ. 25.07.2018. Bull. № 14. (in Ukrainian).
88. *Aksimentyeva O. I., Konopelnyk O. I., Poliovyi D. O.* Electrooptic phenomena in conjugated polymeric systems based on polyaniline and its derivatives // Computational and Experimental Analysis of Functional Materials. Apple Academic Press: New York, 2017. P. 91−150. DOI: https://doi.org/10.1201/9781315366357
89. *Mu L., Zhou L., Pang J., Xu M., Chen Z., Zhou Y., Wang J., Peng J.* Color reproduction of reflective display based on conjugated electrochromic polymer // Org. Electronics. 2020. Vol. 85. DOI: https://doi.org/10.1016/j.orgel.2020.105850
90. *Late D. J., Liu B., Matte R. H. S. S., Rao C. N. R., Dravid V. P.* Rapid characterization of ultrathin layers of chalcogenides on SiO_2/Si substrates // Adv. Funct. Mater. 2012. Vol. 22. P. 1894−1905. DOI: https://doi.org/10.1002/adfm.201102913
91. *Hu P. A., Wen Z., Wang L., Tan P., Xiao K.* Synthesis of few-layer GaSe nanosheets for high performance photodetectors // ACS Nano. 2012. Vol. 6. P. 5988−5994. DOI: https://doi.org/10.1021/nn300889c
92. *Gautam U. K., Vivekchand S. R. C., Govindaraj A., Kulkarni G. U., Selvi N. R., Rao C. N. R.* Generation of onions and nanotubes of GaS and GaSe through laser and thermally induced exfoliation // J. Amer. Chem Soc. 2005. Vol. 127. P. 3658−3659. DOI: https://doi.org/10.1021/ja042294k
93. *Chikan V., Kelley D. F.* Synthesis of highly luminescent GaSe nanoparticles // NanoLett. 2002. Vol. 2. P. 141−145. DOI: https://doi.org/10.1021/nl015641m
94. *Aksimentyeva O. I., Demchenko P. Yu., Savchyn V. P., Balitskii O. A.* Structure, electrical and luminescent properties of the polyaniline–GaSe hybrid nanocomposites // Mol. Cryst. Liq. Cryst. 2011. Vol. 536. P. 297−303. DOI: https://doi.org/10.1080/15421406.2011.538345
95. *Balyts'kyi O. O.* Fracture of layered gallium and indium chalcogenides // Mater. Sci. 2005. Vol. 41. P. 839−842. DOI: https://doi.org/10.1007/s11003-006-0050-4
96. *Aksimentyeva O. I., Demchenko P. Yu., Savchyn V. P., Balitskii O. A.* To the chemical exfoliation phenomena during layered GaSe-polyaniline interaction // Nanoscale Res. Lett. 2013. Vol. 8. DOI: https://doi.org/10.1186/1556-276X-8-29

WELLCOME
on 3rd International Research And Practice Conference "Nanoobjects & Nanostructuring" (N&N–2024)
September 2024
Lviv, Ukraine